European Journal of Medicinal Chemistry 214 (2021) 113248

Contents lists available at ScienceDirect

European Journal of Medicinal Chemistry

journal homepage: http://www.elsevier.com/locate/ejmech

Potent and orally bioavailable CDK8 inhibitors: Design, synthesis, structure-activity relationship analysis and biological evaluation

Mingfeng Yu [a], Theodosia Teo [a], Yuchao Yang [a], Manjun Li [a], Yi Long [a], Stephen Philip [a], Benjamin Noll [a], Gary K. Heinemann [a], Sarah Diab [a], Preethi Eldi [b], Laychiluh Mekonnen [a], Abel T. Anshabo [a], Muhammed H. Rahaman [a], Robert Milne [a], John D. Hayball [b], Shudong Wang [a, *]

[a] Drug Discovery and Development, Cancer Research Institute, Clinical and Health Sciences, University of South Australia, Adelaide, South Australia, 5000, Australia

[b] Experimental Therapeutics, Cancer Research Institute, Clinical and Health Sciences, University of South Australia, Adelaide, South Australia, 5000, Australia

ARTICLE INFO

Article history:
Received 21 December 2020
Received in revised form
23 January 2021
Accepted 24 January 2021
Available online 3 February 2021

Keywords:
CDK8 inhibitor
Structure-activity relationship
Drug-like properties
Pharmacokinetics
Toxicity

ABSTRACT

CDK8 regulates transcription either by phosphorylation of transcription factors or, as part of a four-subunit kinase module, through a reversible association of the kinase module with the Mediator complex, a highly conserved transcriptional coactivator. Deregulation of CDK8 has been found in various types of human cancer, while the role of CDK8 in supressing anti-cancer response of natural killer cells is being understood. Currently, CDK8-targeting cancer drugs are highly sought-after. Herein we detail the discovery of a series of novel pyridine-derived CDK8 inhibitors. Medicinal chemistry optimisation gave rise to **38** (AU1-100), a potent CDK8 inhibitor with oral bioavailability. The compound inhibited the proliferation of MV4-11 acute myeloid leukaemia cells with the kinase activity of cellular CDK8 dampened. No systemic toxicology was observed in the mice treated with **38**. These results warrant further pre-clinical studies of **38** as an anti-cancer agent.

1. Introduction

Cyclin-dependent kinases (CDKs) in partnership with their respective cognate cyclins orchestrate a wide range of cardinal regulatory events, but particularly cell division and transcription [1]. Originally discovered as a putative kinase partner of cyclin C [2,3], CDK8 is a ubiquitously expressed, primarily transcriptional member of the CDK family [4]. The kinase controls gene expression by phosphorylation of transcription factors including neurogenic locus notch homolog proteins (NOTCH) [5], mothers against decapentaplegic homologs (SMADs) [6], sterol regulatory element-binding protein 1C (SREBP-1C) [7] and signal transducer and activator of transcription 1 (STAT1) [8]; the phosphorylation either directly tunes the activity of these transcription factors or primes them for ubiquitin-mediated proteasomal degradation. Alternatively, as part of a four-subunit kinase module that additionally comprises cyclin C, MED12 and MED13 [9], CDK8 regulates transcription through a reversible association of the kinase module with the Mediator complex, a highly conserved transcriptional coactivator that serves as a "molecular bridge" to transfer regulatory signals from DNA-binding transcription factors directly to the RNA polymerase II preinitiation complex [10].

Given the pivotal regulatory role of CDK8 in transcription, it is hardly surprising that its deregulation is implicated in multiple types of human cancer. The CDK8-coding gene was conferred an oncogene status first in colorectal cancer in 2008 [11]. Since then, the kinase activity of CDK8 has been found oncogenic in melanoma [12], breast cancer [13], acute myeloid leukaemia (AML) [14], pancreatic cancer [15], prostate cancer [16], and so forth [17]. In addition, a previous study has shown that CDK8 kinase activity attenuates the defence of natural killer cells against malignant cells and restrains the tumour surveillance of the former cells [18]; this concept has been further validated both genetically (*via* deletion of the CDK8-coding gene in natural killer cells) [19] and pharmacologically (by use of several exogenous small-molecule inhibitors of CDK8) [20]. Taken together, these studies provide a rationale for the

* Corresponding author.
E-mail address: shudong.wang@unisa.edu.au (S. Wang).

https://doi.org/10.1016/j.ejmech.2021.113248
0223-5234/

potential application of pharmacological inhibition of CDK8 as a strategy for cancer therapy. Accordingly, there is a pressing demand in discovering potent and selective small-molecule CDK8 inhibitors.

Since the report of cortistatin A (Fig. 1) as a high-affinity ligand of CDK8 in 2009 [21], diverse scaffolds, either naturally derived or chemically synthesised, have been exploited in search of CDK8 inhibitors. The known CDK8 inhibitors include, but are not limited to, senexin B [22], CCT251545 [23,24], MSC253818 [25], SEL120-34A [26], W-34 [27], T-418 [28], and derivatives of steroid [29,30], 1,6-naphthyridine [31], thieno[2,3-*c*]pyridine [32], 4-(1*H*-pyrrol-4-yl)pyridine [33], pyrido[2,3-*b*][1,5]benzoxazepin-5(6*H*)-one [34] (Fig. 1). These compounds inhibit CDK8 at low nanomolar concentrations, and two of them have advanced into phase I clinical trials—senexin B (BCD-115) and SEL120-34A (SEL120) for treatments of local advanced and metastatic breast cancer with estrogen receptor-positive/human epidermal growth factor receptor 2-negative (NCT03065010, completed with no results released yet), and of AML or high-risk myelodysplastic syndrome (NCT04021368, recruiting patients), respectively (ClinicalTrials.gov, last accessed 21st December 2020).

Our earlier attempt to identify novel CDK8 inhibitor scaffolds through virtual screening gave rise to a total of 476 hits prior to visual inspection and subsequent selection for biological validation [35]. Several classes of scaffolds dominated the results, including 4-substituted quin(az)olines, 1,3-diarylureas, and multi-substituted pyridines. While structural optimisation of the first two chemical series for potency, selectivity and drug-like properties is underway, we report herein our progress on developing pyridine-derived CDK8 inhibitors.

2. Results and discussion

2.1. Rational design of 3,4,5-trisubstituted pyridines

In 2015, an elegant study was published on the discovery of CCT251545 (Fig. 1), a 3,4,5-trisubstituted pyridine derivative, as a potent and selective CDK8 inhibitor [24]. This discovery in combination with our virtual screening results (*vide supra*) not only boosted our confidence in seeking pyridine-derived CDK8 inhibitors but also offered a reasonable starting point for medicinal chemistry optimisation.

An analysis of the X-ray crystal structure of CCT251545 bound to CDK8/cyclin C (Fig. 2) [24] assisted in our rational design of novel CDK8 inhibitors: (I) The pyridine core acts as a hinge binder, with its nitrogen atom forming a hydrogen bond with the NH of Ala100. An interaction of this kind had been considered typical of CDK8 inhibitors yet with distinct chemical scaffolds [14,24,36], so the pyridine core was retained in our structural optimisation. (II) The proper size and orientation of the chlorine atom at the pyridine-C3 position (Fig. 1) permit a Cl-π interaction [37] with the gatekeeper residue Phe97 (Fig. 2), and therefore this atom remained

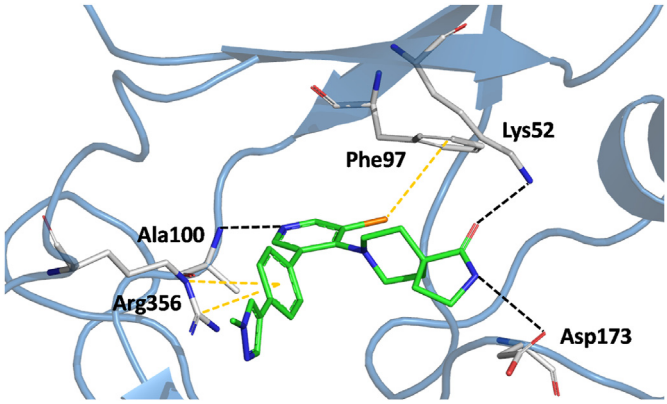

Fig. 2. X-ray crystal structure of CCT251545 bound to CDK8/cyclin C (PDB ID: 5BNJ). CCT251545 is engaged in three hydrogen bonds (black dotted lines) as well as π-cation and Cl-π interactions (yellow dotted lines) with CDK8. The kinase is depicted as sky blue ribbons. Nitrogen atoms are shown in royal blue, oxygen atoms in red, receptor carbon atoms in grey, ligand carbon atoms in green, and the chlorine atom is coloured orange. The illustration was generated using PyMOL Molecular Graphics System Version 2.4.0 Schrödinger, LLC.

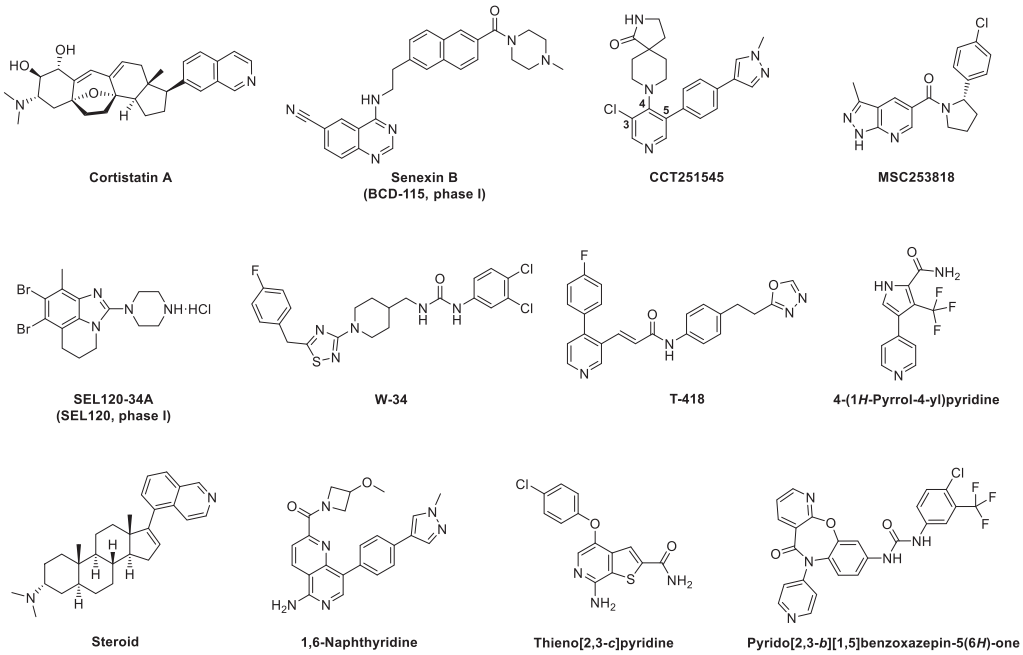

Fig. 1. Chemical structures of selected CDK8 inhibitors.

unchanged. (III) The amide of the spirolactam moiety at the pyridine-C4 position bridges Lys52 and Asp173 through two hydrogen bonds. We envisaged that a replacement of this moiety with a heteroaromatic ring appended with an amide arm could maintain, if not strengthen, the contact with both amino acids. (IV) While the phenyl ring at the pyridine-C5 position forms a π-cation interaction with Arg356, the entire 4-(1-methyl-1*H*-pyrazol-4-yl) phenyl moiety occupies the solvent-exposed region, an element of the kinase structure that has the capacity to tolerate structural modifications and is thus often exploited for structure-based drug design [38]. As a result, our medicinal chemistry optimisation of CCT251545 focused on C4 and C5 positions of the pyridine ring.

Modification at the Pyridine-C4 Position. The hydrogen bonding of the 2,8-diazaspiro[4.5]decan-1-one moiety to Lys52 and Asp173 contributes to the high affinity of CCT251545 for CDK8 (Fig. 2). In fact, both amino acids are conserved across the CDK family [39]. As such, we hypothesised that the moieties at the pyrimidine-C4 position of our previously synthesised CDK inhibitors [40–48] that were capable of interacting with either or both counterparts of CDK8-Lys52/Asp173 in alternative CDKs could stand a chance of replacing the 2,8-diazaspiro[4.5]decan-1-one group of CCT251545 at no cost of CDK8 inhibitory potency. With this in mind, we revisited our in-house library of co-crystal structures of small-molecule inhibitors in complex with CDKs, and found several functionalised five-membered aromatic moieties formed hydrogen bonds with CDK2-Asp145 or CDK9-Asp167 [41,42,45]; two equivalents of CDK8-Asp173 [39]. One of such moieties was 1*H*-pyrrol-4-yl, but a survey of the relevant literature revealed that this moiety in the context of the pyridine core had been claimed in a patent application [49] (Fig. 3). To circumvent this, we altered the topology of the pyrrole-pyridine system, linking the former to the latter *via* the N1′-C4 bond instead, with a view to contacting CDK8-Asp173 by an exocyclic carboxylic acid or amide arm (part I, Fig. 3).

Optimisation at the Pyridine-C5 Position. The 4-(1-methyl-1*H*-pyrazol-4-yl)phenyl pendant of CCT251545 nestles in the solvent channel that typically tolerates structural modifications (Fig. 2). A literature survey of the chemical structures containing a spirolactam-pyridine core unveiled that reversing the topology of the phenyl-pyrazole pendant at the pyridine-C5 position remained unexplored and, more importantly, that replacing this pendent with fused ring systems was underexplored. Accordingly, we explored chemical space along both lines, with the common aim of enhancing the π-cation interaction with CDK8-Arg356 by introduction of electron-rich substituents (part II, Fig. 3).

2.2. Chemistry

The synthetic route deployed to prepare 3-chloro-5-(4-(1-methyl-1*H*-pyrazol-4-yl)phenyl)-4-(3-substituted-1*H*-pyrrol-1-yl)pyridines **8**–**10** is delineated in Scheme 1. *In situ* mono-lithiation at the C4 position of 3-bromo-5-chloropyridine **1** with lithium diisopropylamide (LDA) at −78 °C was followed by an exchange with a chlorine from hexachloroethane, giving 3-bromo-4,5-dichloropyridine **2** in 65% yield. This newly introduced chlorine was further displaced with methyl 1*H*-pyrrole-3-carboxylate under microwave irradiation in the presence of caesium carbonate to afford methyl 1-(3-bromo-5-chloropyridin-4-yl)-1*H*-pyrrole-3-carboxylate **3** in a yield of 48%. In parallel, starting from 1-chloro-4-iodobenzene **4**, two halogen atoms—iodine and chlorine—were successively replaced with 1-methyl-1*H*-pyrazol-4-yl and 4,4,5,5-tetramethyl-1,3,2-dioxaborolan-2-yl, respectively, using two palladium-catalysed reactions: a Suzuki coupling with the iodine using Pd(dppf)$Cl_2 \cdot CH_2Cl_2$, and a Miyaura borylation of the chlorine employing a combination of $Pd_2(dba)_3$ with XPhos. Both reactions were carried out in the presence of a base at an elevated temperature overnight, resulting in 1-methyl-4-(4-(4,4,5,5-tetramethyl-1,3,2-dioxaborolan-2-yl)phenyl)-1*H*-pyrazole **6** in a good overall yield (**5**: 58% and **6**: 83%). A second Suzuki coupling of bromide **3** with boronate ester **6** using the same palladium catalyst yet under microwave irradiation for a much shorter time (*i.e.*, 1 h) gave methyl 1-(3-chloro-5-(4-(1-methyl-1*H*-pyrazol-4-yl) phenyl)pyridin-4-yl)-1*H*-pyrrole-3-carboxylate **7** in 67% yield, which was subsequently subjected to saponification in an alkaline

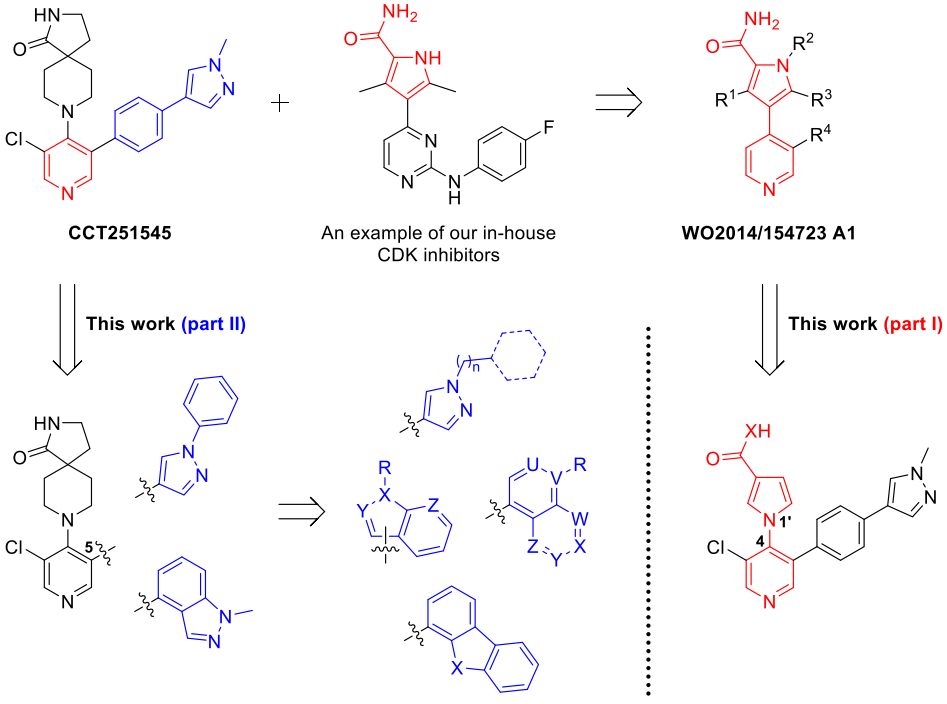

Fig. 3. Design of novel chemical scaffolds for CDK8 inhibitors.

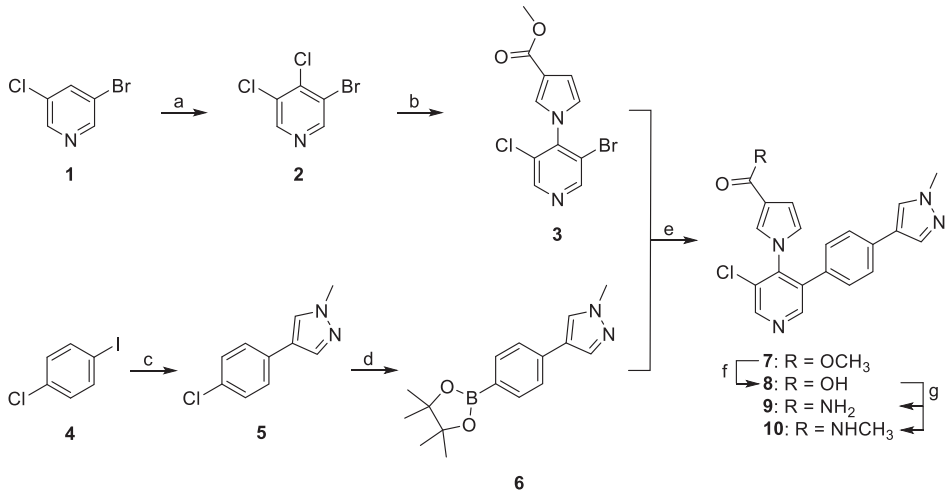

Scheme 1. Synthesis of 3-chloro-5-(4-(1-methyl-1*H*-pyrazol-4-yl)phenyl)-4-(3-substituted-1*H*-pyrrol-1-yl)pyridines **8**–**10**. *Reagents and conditions*: (a) (1) LDA (2.0 M in THF/heptane/ethylbenzene), THF, −78 °C, 1 h; (2) hexachloroethane, THF, −78 °C, 1 h, 65%; (b) methyl 1*H*-pyrrole-3-carboxylate, Cs_2CO_3, 1,4-dioxane, microwave 150–300 W, 200 °C, 1 h, 48%; (c) 1-methyl-4-(4,4,5,5-tetramethyl-1,3,2-dioxaborolan-2-yl)-1*H*-pyrazole, Pd(dppf)Cl_2·CH_2Cl_2, Na_2CO_3, THF/H_2O, 80 °C, o/n, 58%; (d) bis(pinacolato)diboron, $Pd_2(dba)_3$, XPhos, potassium acetate, 1,4-dioxane, 85 °C, o/n, 83%; (e) Pd(dppf)Cl_2·CH_2Cl_2, 0.5 M Na_2CO_3, CH_3CN, microwave 150–300 W, 120 °C, 1 h, 67%; (f) 1 M NaOH, CH_3OH, reflux, 2 h, 95%; (g) NH_3 (0.5 M in 1,4-dioxane) or CH_3NH_2·HCl, HATU, DIPEA, DMF, 0 °C to rt, o/n, **9**: 73%, **10**: 70%.

methanolic solution at reflux to yield carboxylic acid **8** in a yield of 95%. Finally, amination of carboxylic acid **8** with either ammonia or methylamine hydrochloride was effected by 1-[bis(dimethylamino) methylene]-1*H*-1,2,3-triazolo[4,5-*b*]pyridinium 3-oxid hexafluoro phosphate (HATU), a coupling reagent, in the presence of *N*,*N*-diisopropylethylamine (DIPEA) in anhydrous *N*,*N*-dimethylformamide (DMF), giving the corresponding amides **9** and **10** in good yields (**9**: 73% and **10**: 70%).

The above synthetic approach was successfully applied to the preparation of 8-(3-chloro-5-substituted-pyridin-4-yl)-2,8-diazaspiro[4.5]decan-1-ones with a single exception of 8-(3-chloro-5-((1-methyl-1*H*-indazol-5-yl)amino)pyridin-4-yl)-2,8-diazaspiro[4.5]decan-1-one **12** that was synthesised *via* $Pd_2(dba)_3$/Xantphos-catalysed Buchwald-Hartwig amination (Scheme 2). In brief, 3-bromo-4,5-dichloropyridine **2** sequentially underwent nucleophilic aromatic substitution with *tert*-butyl 1-oxo-2,8-diazaspiro[4.5]decane-8-carboxylate, and Pd(dppf)Cl_2·CH_2Cl_2-catalysed Suzuki coupling with diverse aromatic boronic acids or boronate esters, affording desired 8-(3-chloro-5-aryl-pyridin-4-yl)-2,8-diazaspiro[4.5]decan-1-ones **13**–**34**, **36** and **38**–**41** in varying yields (13–69%). Among them, **34** and **36** were further deprotected using lithium hydroxide in a mixture of tetrahydrofuran (THF) and methanol to yield the corresponding (aza)indoles **35** and **37** with an intact NH site, respectively (**35**: 80% and **37**: 75%).

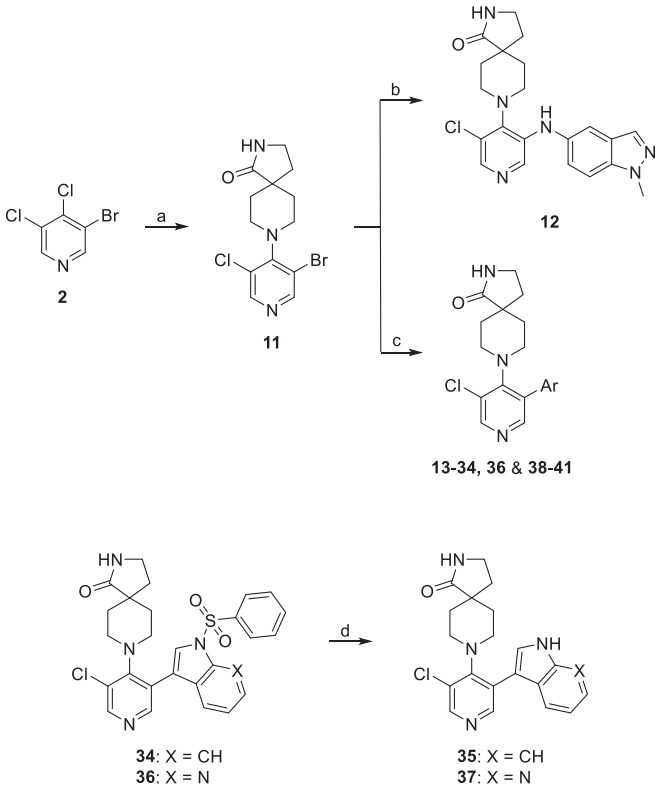

Scheme 2. Synthesis of 8-(3-chloro-5-substituted-pyridin-4-yl)-2,8-diazaspiro[4.5]decan-1-ones **12**–**41**. *Reagents and conditions*: (a) *tert*-butyl 1-oxo-2,8-diazaspiro[4.5]decane-8-carboxylate, triethylamine, 1-methoxy-2-propanol, microwave 150–300 W, 220 °C, 2.5 h, 79%; (b) 1-methyl-1*H*-indazol-5-amine, $Pd_2(dba)_3$, Xantphos, Cs_2CO_3, 1,4-dioxane, microwave 150–300 W, 180 °C, 1 h, 25%; (c) appropriate boronic acid or boronate ester, Pd(dppf)Cl_2·CH_2Cl_2, 0.5 M Na_2CO_3, CH_3CN, microwave 150–300 W, 120–140 °C, 1 h, 13–69%; (d) LiOH, THF/CH_3OH, 50 °C, 1 h, **35**: 80%, **37**: 75%.

2.3. Structure-activity relationship analysis

Pharmacological inhibition of CDK8 upregulated the super-enhancer-associated genes with tumour-suppressing and lineage-controlling functions in a range of AML cell lines, particularly MV4-11 [14]. Hence, this cell line was selected to evaluate the cytotoxicity of our newly synthesised compounds. The evaluation was conducted in-house by means of a cell viability assay using resazurin [50], and CDK8 inhibitory potency of the compounds measured with a radiometric kinase assay using [γ-^{33}P]-ATP (also known as ^{33}PanQinase® Activity Assay) at ProQinase GmbH.

Nanomolar inhibitors of CDK8 were successfully derived from the pyrrole(C4′)-pyridine(C4) system (see an example of 4-(1*H*-pyrrol-4-yl)pyridines in Fig. 1) [33]. However, in our work, three prototype molecules **8**–**10** with a pyrrole(N1′)-pyridine(C4) skeleton failed to achieve nanomolar CDK8 inhibitory activity (Table 1), which could be attributed to unfavourable orientations of carboxylic acid/amide pendants for the binding to the kinase. As

Table 1
Chemical structures and biological activities of **8**–**10**.

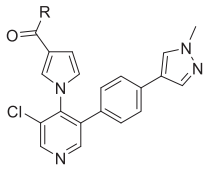

8-10

Compound	R	CDK8/cyclin C inhibition, K_i (μM)[a]	MV4-11 anti-proliferation, GI_{50} (μM)[b]
8	OH	4.19	87.07 ± 9.02
9	NH_2	1.09	9.58 ± 1.12
10	$NHCH_3$	2.03	34.96 ± 6.94

[a] Inhibition of CDK8/cyclin C was measured with a radiometric kinase assay using [γ-^{33}P]-ATP (also known as ^{33}PanQinase® Activity Assay) at ProQinase GmbH, and the K_m value used as the ATP concentration. Each apparent inhibition constant (K_i) was calculated using the corresponding IC_{50} value and the K_m (ATP) value. [b] GI_{50} values were determined in-house by a 72-h resazurin assay, and are presented as mean ± standard deviation derived from at least two replicates.

Table 2
Chemical structures and biological activities of **13**–**16**.

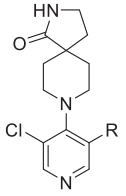

13-16

Compound	R	CDK8/cyclin C inhibition, K_i (μM)[a]	MV4-11 anti-proliferation, GI_{50} (μM)[b]
13	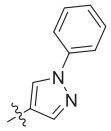	0.042	0.84 ± 0.11
14	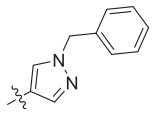	0.346	5.34 ± 0.92
15	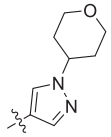	0.124	7.43 ± 1.39
16	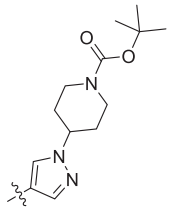	0.700	12.20 ± 3.87
CCT251545	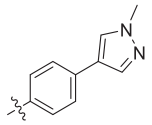	0.009	0.03 ± 0.02

[a] Inhibition of CDK8/cyclin C was measured with a radiometric kinase assay using [γ-^{33}P]-ATP (also known as ^{33}PanQinase® Activity Assay) at ProQinase GmbH, and the K_m value used as the ATP concentration. Each apparent inhibition constant (K_i) was calculated using the corresponding IC_{50} value and the K_m (ATP) value. [b] GI_{50} values were determined in-house by a 72-h resazurin assay, and are presented as mean ± standard deviation derived from at least two replicates.

Table 3
Chemical structures and biological activities of **12** and **17**–**30**.

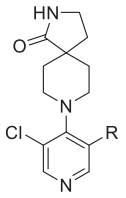

12 & **17-30**

Compound	R	CDK8/cyclin C inhibition, K_i (μM)[a]	MV4-11 anti-proliferation, GI_{50} (μM)[b]
12	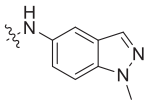	0.670	1.71 ± 0.96
17	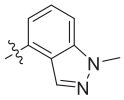	0.458	27.66 ± 5.07
18	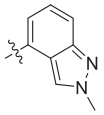	0.052	5.26 ± 0.54
19	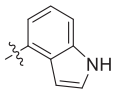	0.019	1.91 ± 1.35
20	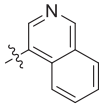	0.066	7.55 ± 0.76
21	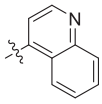	0.138	53.46 ± 10.33
22	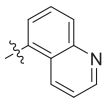	0.022	3.65 ± 0.74
23	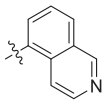	0.052	62.31 ± 3.31
24	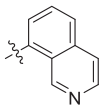	3.140	64.17 ± 8.08
25	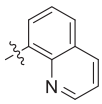	0.114	9.15 ± 0.86
26	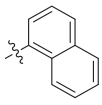	0.016	0.82 ± 0.09
27	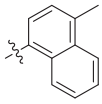	0.022	0.71 ± 0.12

Table 3 (*continued*)

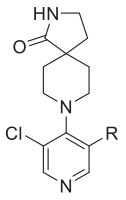

12 & **17-30**

Compound	R	CDK8/cyclin C inhibition, K_i (μM)[a]	MV4-11 anti-proliferation, GI_{50} (μM)[b]
28	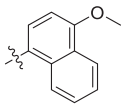	0.026	33.16 ± 2.29
29	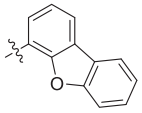	0.016	6.68 ± 0.18
30	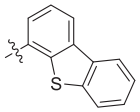	0.024	6.35 ± 0.35
CCT251545	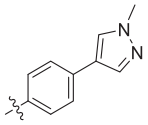	0.009	0.03 ± 0.02

[a] Inhibition of CDK8/cyclin C was measured with a radiometric kinase assay using [γ-^{33}P]-ATP (also known as ^{33}PanQinase® Activity Assay) at ProQinase GmbH, and the K_m value used as the ATP concentration. Each apparent inhibition constant (K_i) was calculated using the corresponding IC_{50} value and the K_m (ATP) value. [b] GI_{50} values were determined in-house by a 72-h resazurin assay, and are presented as mean ± standard deviation derived from at least two replicates.

expected, these three compounds exerted little anti-proliferative effect on MV4-11 cells.

Our attention was then turned to diversification of the substituent at the pyridine-C5 position of CCT251545 (Tables 2–4). As a positive control, CCT251545 was first synthesised in-house and evaluated, showing high inhibitory activity towards CDK8 ($K_i = 0.009$ μM) and potent anti-proliferative effect on MV4-11 cells ($GI_{50} = 0.03$ μM) (Table 2). The former value is in agreement with the reported data [24,51], whereas there is, to the best of our knowledge, no literature value of the latter.

Reversing the topology of the phenyl-pyrazole pendant of CCT251545 gave rise to **13**, which was slightly less inhibitory to CDK8, but maintained a low-nanomolar potency ($K_i = 0.042$ μM) (Table 2). The anti-proliferative effect of **13** was just within the sub-micromolar concentration range ($GI_{50} = 0.84$ μM). Spacing the two components of the reversed pendant with a methylene (*i.e.*, **14**) further reduced kinase inhibitory activity as well as cellular potency, and so did replacing the phenyl component with a less rigid aliphatic heterocycle (*i.e.*, a tetrahydropyran in **15** and a piperidine in **16**). These three compounds showed high sub-micromolar and micromolar inhibitory activities against CDK8 and MV4-11 cells, respectively ($K_i = 0.124–0.700$ μM and $GI_{50} = 5.34–12.20$ μM). These results suggested that an increased flexibility of the substituent at the pyridine-C5 position could be detrimental to inhibition of both CDK8 kinase activity and MV4-11 cell growth. To diminish the flexibility, we switched to incorporate a wide range of fused aromatic rings onto this position. Among them were [5,6]-, [6,5]-, [6,6]- and [6,5,6]-membered-membered bi-/tri-cyclic fused moieties (Tables 3 and 4).

Direct amalgamation of the phenyl with the *N*-methylpyrazolyl within CCT251545 formed two *N*-methylindazol-4-yl-containing compounds **17** and **18**, with inhibition of CDK8 and MV4-11 cells weakened to an extent that was contingent on the orientation of the methyl group (**17** [*N*(1)-methyl]: $K_i = 0.458$ μM and $GI_{50} = 27.66$ μM versus **18** [*N*(2)-methyl]: $K_i = 0.052$ μM and $GI_{50} = 5.26$ μM) (Table 3). Bridging the *N*(1)-methylindazolyl pendant and the pyridine core with a secondary amino group deteriorated the kinase inhibition (*i.e.*, **12**: $K_i = 0.670$ μM), so no alternative single-heteroatom linkers were further attempted. Replacing the N(2)-CH_3 site of the *N*(2)-methylindazol-4-yl with CH afforded **19** appended with a 1*H*-indol-4-yl, and returned a higher affinity for CDK8 ($K_i = 0.019$ μM) and a more potent growth inhibition of MV4-11 cells ($GI_{50} = 1.91$ μM). Expanding the indole ring with an additional carbon gave rise to a range of (iso) quinoline-based pendants (*i.e.*, **20**–**25**) with varying degrees of CDK8 inhibitory potency, indicating the position of the only nitrogen atom played an important role. Detailedly, **22** with a quinolin-5-yl was the most active against CDK8 ($K_i = 0.022$ μM), whereas **24** with an isoquinolin-8-yl hardly suppressed the kinase activity ($K_i = 3.140$ μM). The rest were sub-micromolar inhibitors of CDK8 ($K_i = 0.052–0.138$ μM). All of the (iso)quinoline-containing compounds **20**–**25** dampened the proliferation of MV4-11 cells at micromolar concentrations (*i.e.*, $GI_{50} = 3.65–64.17$ μM). Removal of the sole nitrogen atom from (iso)quinolines furnished **26** with a naphthalen-1-yl, and further introduction of a methyl or methoxy group at the naphthalene-C4 position gave **27** and **28**, respectively. These three molecules inhibited CDK8 kinase activity at low two-digit nanomolar concentrations ($K_i = 0.016–0.026$ μM), which were translated into their sub-micromolar anti-proliferative effects on MV4-11 cells with the exception of **28** ($GI_{50} = 0.82$, 0.71 and 33.16 μM for **26**, **27** and **28**, respectively). Again, another poor correlation between CDK8 inhibition and MV4-11 anti-proliferation was found for **29** and **30** with bulkier, tricyclic fused pendants. Both compounds

Table 4
Chemical structures and biological activities of **31**–**41**.

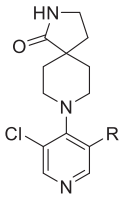

31-41

Compound	R	CDK8/cyclin C inhibition, K_i (μM)[a]	MV4-11 anti-proliferation, GI_{50} (μM)[b]
31	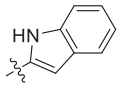	0.156	6.84 ± 0.90
32	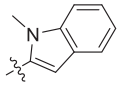	0.079	10.06 ± 3.78
33	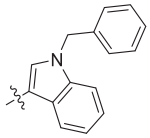	0.058	30.59 ± 8.63
34	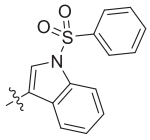	0.645	28.44 ± 4.52
35	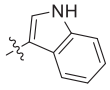	0.056	8.77 ± 2.04
36	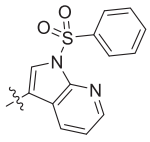	1.300	40.16 ± 2.50
37	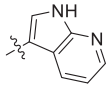	0.050	7.82 ± 1.20
38	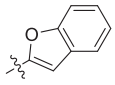	0.014	0.36 ± 0.35
39	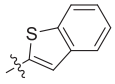	0.014	0.58 ± 0.14
40	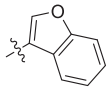	0.048	29.16 ± 1.19
41	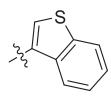	0.021	0.35 ± 0.22
CCT251545	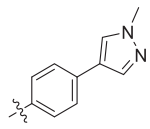	0.009	0.03 ± 0.02

[a] Inhibition of CDK8/cyclin C was measured with a radiometric kinase assay using [γ-^{33}P]-ATP (also known as ^{33}PanQinase® Activity Assay) at ProQinase GmbH, and the K_m value used as the ATP concentration. Each apparent inhibition constant (K_i) was calculated using the corresponding IC_{50} value and the K_m (ATP) value. [b] GI_{50} values were determined in-house by a 72-h resazurin assay, and are presented as mean ± standard deviation derived from at least two replicates.

suppressed CDK8 kinase activity potently (K_i = 0.016 and 0.024 μM), but induced marginal toxicity towards MV4-11 cells (GI_{50} = 6.68 and 6.35 μM).

Two out of three most potent CDK8 inhibitors identified thus far were **19** and **29** (Tables 1–3), where a five-membered ring was attached to the pyridine core through its fused six-membered ring (*i.e.*, phenyl in both cases). This observation led us to consider and test the possibility of improving CDK8 inhibitory activity by diverting a connecting site onto a fused five-membered aromatic ring instead (Table 4). Two such counterparts of **19** were first prepared, with connecting sites of **31** and **35** located at their respective C2 and C3 positions of the common indole ring. Both counterparts were weaker inhibitors of CDK8 and MV4-11 cells than **19** (**31**: K_i = 0.156 μM and GI_{50} = 6.84 μM; **35**: K_i = 0.056 μM and GI_{50} = 8.77 μM). As expected, protecting the indole-NH of **35** with a sizeable benzenesulfonyl group greatly decreased inhibition of both the kinase and cells (**34**: K_i = 0.645 μM and GI_{50} = 28.44 μM). The same held true for the pair of 7-azaindole (**37**: K_i = 0.050 μM and GI_{50} = 7.82 μM) and its *N*(1)-benzenesulfonyl-protected form (**36**: K_i = 1.300 μM and GI_{50} = 40.16 μM). These findings were consistent with our previous observation that flexible substituents might not be favourable at the pyridine-C5 position (Table 2). In contrast, masking the indole-NH of **35** with a large-size benzyl group maintained CDK8 inhibitory activity (**33**: K_i = 0.058 μM versus **35**: K_i = 0.056 μM) (Table 4). Similarly, substitution of the indole-NH of **31** with a small-size methyl group even ameliorated the potency against the kinase (**32**: K_i = 0.079 μM versus **31**: K_i = 0.156 μM). Both cases implied that an intact indole-NH might not be essential for CDK8 inhibitory activity. As a result, benzofuranyl and benzothiophenyl moieties, where their respective oxygen and sulphur atoms are isosteres of the indole-NH, were selected to replace the indolyl pendant. Among the four compounds thus synthesised, **38**, **39** and **41** formed a group of inhibitors with the highest affinity for CDK8 as well as with the greatest effectiveness against MV4-11 cells. Specifically, K_i values of **38**, **39** and **41** were determined to be 0.014, 0.014, and 0.021 μM, respectively, all of which were comparable to that of CCT251545 (K_i = 0.009 μM); their respective GI_{50} values of 0.36, 0.58, and 0.35 μM were about one order of magnitude higher than that of the control (GI_{50} = 0.03 μM). Surprisingly, the remaining compound **40** was slightly less active towards CDK8 (K_i = 0.048 μM), but barely suppressed the proliferation of MV4-11 cells (GI_{50} = 29.16 μM).

2.4. Kinase inhibitory selectivity of 38 and 39

To understand kinase inhibitory selectivity of newly synthesised CDK8 inhibitors, the two most potent molecules **38** and **39** were selected and tested against, as a first step, a wide range of other CDK family members at a compound concentration of 1 μM (Fig. 4, below dotted lines). None of the CDKs tested were deprived of more than 50% kinase activity by either compound, with the exceptions of CDKs 1 and 9 in the presence of **38**. Their respective K_i values were later determined to be 1.895 and 1.765 μM, both of which were more than two orders of magnitude higher than that of CDK8 (*i.e.*, 0.014 μM). These results demonstrated that both CDK8 inhibitors were highly selective across the CDK family. Further profiling of kinase inhibitory selectivity included a screening against a wider panel of 47 additional human kinases known to be frequently targeted by CDK inhibitors (Fig. 4, above dotted lines). The activities of only three kinases—the two isoforms of glycogen synthase kinase-3 (GSK-3α/β) and protein kinase C-theta (PCK-θ)—were inhibited more than 50% by both **38** and **39** at 1 μM. The affinities of both compounds for GSK-3α/β were comparable to those for CDK8, with K_i values ranging from 0.004 to 0.043 μM, whereas their inhibitory effects on the kinase activity of PCK-θ were approximately one order of magnitude lower than those of CDK8 (K_i = 0.109 and 0.134 μM versus 0.014 and 0.014 μM, respectively) (Table 5). These three off-targets were expected because CCT251545 had been found to inhibit all of them [52]—to a lesser extent towards GSK-3α/β but to a higher degree towards PCK-θ in comparison with **38** and **39**.

2.5. In vitro anti-proliferative spectra of 38 and 39

As described in Section 2.3, **38** and **39** exerted sub-micromolar anti-proliferative effects on MV4-11 cells. To define the scope of such action, both compounds were further screened against 18 human cancer cell lines (originating in blood/bone marrow, colon/rectum, pancreas, ovary and breast) and one non-transformed cell line (*i.e.*, normal human diploid lung fibroblasts WI-38) (Table 6). Among them, U-937 and MOLM-13 AML cell lines were the most sensitive to **38** and **39**, with GI_{50} values varying from 1.36 to 6.18 μM, but both less amenable than MV4-11 cell line (GI_{50} = 0.36 and 0.58 μM for **38** and **39**, respectively). Greater anti-proliferative effects of both compounds on MV4-11 than on MOLM-13 were in agreement with higher expression of CDK8 in the former cell line (Fig. S1). While GI_{50} values for the majority of solid tumour cell lines spanned from 16.18 to 44.25 μM, those for the rest were all more than 50 μM. These results indicated that the *in vitro* anti-proliferative effect of **38** and **39** could be cell-type specific, in particular towards some of AML cell lines like MV4-11. Importantly, both compounds imposed little inhibitory effects on non-transformed WI-38 lung fibroblasts, and their GI_{50} values were about two orders of magnitude higher than those for MV4-11 cells, achieving a desirable anti-proliferative selectivity. CCT251545 displayed a similar anti-proliferation profile to those of **38** and **39**; the single exception was the sub-micromolar suppression of the control compound on the growth of PANC-1 pancreatic cancer cells (GI_{50} = 0.55 μM).

2.6. Cellular CDK8 inhibition of 38

Given that MV4-11 cells showed the highest sensitivity towards **38**, this AML cell line was chosen to assess the cellular CDK8 inhibitory potency of the compound. MV4-11 cells were incubated with **38** or CCT251545 for 2 h, and analysed by western blotting (Fig. 5). Treatment with either compound significantly reduced the phosphorylation of serine 727 on STAT1, a known substrate of CDK8 [18,53], at concentrations of their respective 1 × and 5 × GI_{50} values, but barely affected the level of total STAT1. These results confirmed the inhibition of the kinase activity of cellular CDK8 by **38**.

2.7. In Vitro Drug-like properties of 38 and 39

Prior to *in vivo* pharmacokinetic and toxicity studies, drug-like properties of **38** and **39** were evaluated *in vitro*, including physicochemical profiling and ADMET (absorption, distribution, metabolism, excretion and toxicity) screening (Table 7). Lipophilicity of a compound contributes to ADME characteristics of the compound, and distribution coefficient (Log D) is typically used as a measure of lipophilicity [54]. Both **38** and **39** had a Log $D_{7.4}$ value of > 4, suggesting their high lipophilicity. The negative log of the acid dissociation constant (pKa) of a molecule predicts the degree of its ionisation at a particular pH, and affects its solubility and permeability by modulating the distribution of neutral and charged species of the compound [54]. A pKa value of 4.90 for **38** indicated that the compound was 50% protonated at pH 4.90. The aqueous solubility of a compound plays an essential role in determining its absorption from the gastrointestinal tract and ultimately its oral

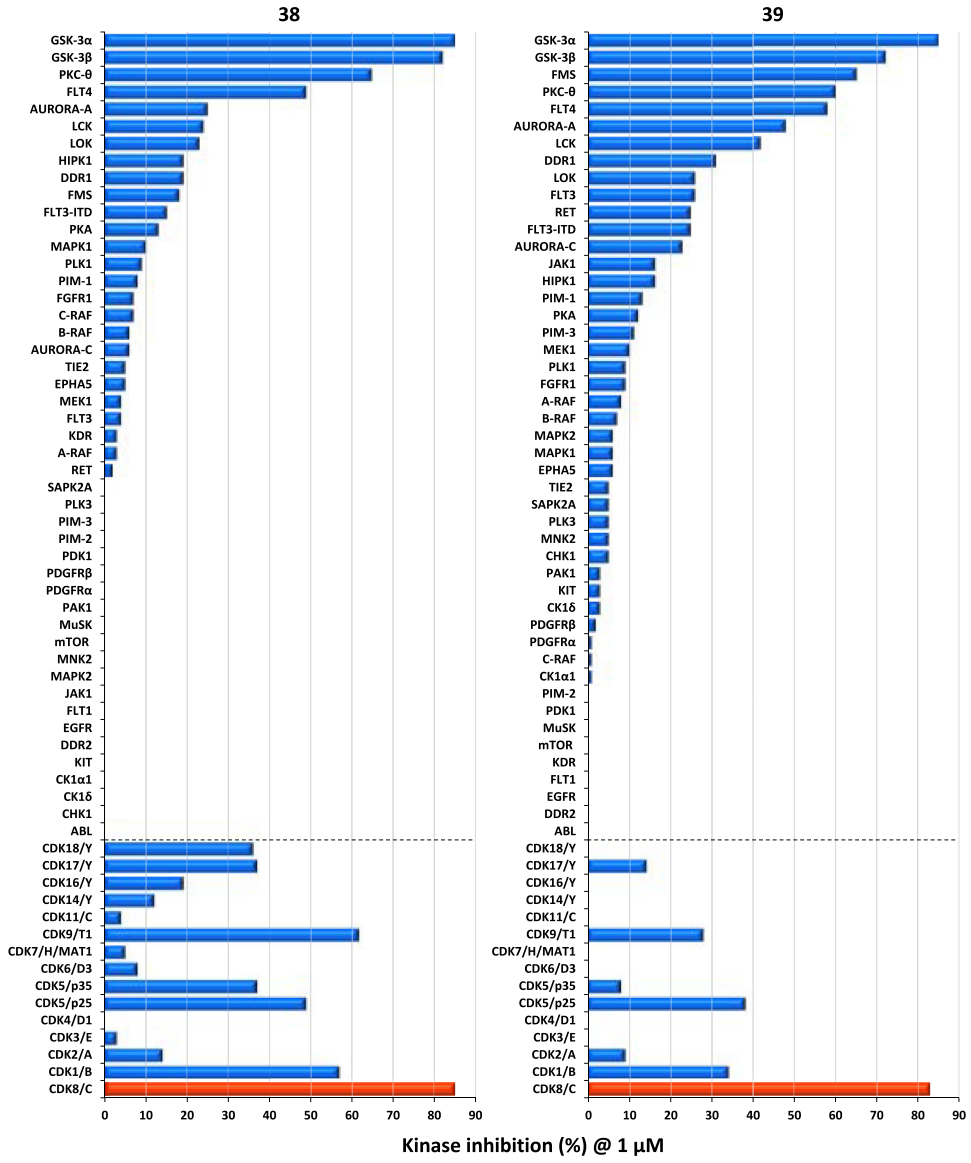

Fig. 4. Kinase inhibition profiles of **38** and **39** (at 1 μM) over a panel of 62 kinases (including 15 CDK/cyclin complexes). The data were acquired at Eurofins Scientific, Reaction Biology Corporation and ProQinase GmbH.

Table 5
Off-targets of **38** and **39**.

Compound	CDK8/cyclin C inhibition, K_i (μM)[a]	Off-target kinase inhibition, K_i (μM)[a]		
		GSK-3α	GSK-3β	PCK-θ
38	0.014	0.013	0.004	0.109
39	0.014	0.043	0.018	0.134
CCT251545	0.009	0.231[b]	0.345[b]	0.061[b]

[a] Inhibition of CDK8/cyclin C was measured at ProQinase GmbH, and GSK-3α/β and PCK-θ were tested at Reaction Biology Corporation. The K_m value was used as the ATP concentration for each kinase. Each apparent inhibition constant (K_i) was calculated using the corresponding IC_{50} and K_m (ATP) values. [b] K_i values were calculated using the IC_{50} values reported in reference [52].

bioavailability [55]. Although a precise measure of aqueous solubility could not be provided by the turbidimetric assay, **38** and **39** with their respective solubility levels of 10—30 and < 20 μM were considered partially soluble. This suboptimal solubility became less concerned because both **38** and **39** displayed high permeability, with their passive apparent permeability coefficient (P_{app}(A—B)) values being more than 20 × 10^{-6} cm/s. Additionally, both efflux ratios of around 1 suggested that neither **38** nor **39** underwent active efflux.

Given that a large portion of kinase inhibitors approved by the United States Food and Drug Administration (US FDA) are engaged in combination cancer therapies [56], the liabilities of **38** and **39** for drug-drug interactions were assessed using a range of cytochrome P450 (CYP450) enzymes; a family of haemoproteins that are involved in the metabolism of drugs [57]. Both compounds exerted no inhibitory effects on CYP2C9, CYP2C19 and CYP2D6 (IC_{50} > 25 μM in all cases), and suppressed CYP3A4 moderately (**38**: IC_{50} = 4.59 μM and **39**: IC_{50} = 2.11 μM). The remaining isoform CYP1A was inhibited quite modestly by **38** (IC_{50} = 7.7 μM), but very

Table 6
Anti-proliferative effects of **38** and **39** on a panel of 20 human cell lines.

Origin	Cancer Cell line	Anti-proliferation, GI_{50} (μM)[a]		
		38	**39**	**CCT251545**
Blood/Bone marrow	HL-60	35.31 ± 4.91	ND[b]	> 50
	Kasumi-1	> 50	ND	37.03[c]
	KG-1	7.13 ± 1.25	ND	19.98 ± 0.89
	KG-1a	19.55[c]	ND	32.71[c]
	MOLM-13	6.18 ± 0.10	5.81 ± 1.35	2.80 ± 0.86
	MV4-11	0.36 ± 0.35	0.58 ± 0.14	0.03 ± 0.02
	NB4	40.80[c]	ND	> 50
	PL-21	25.35[c]	ND	13.76[c]
	THP-1	> 50	ND	> 50
	U-937	1.36 ± 0.21	2.69 ± 0.78	22.44 ± 0.50
Colon/Rectum	COLO 205	> 50	> 50	37.73 ± 8.53
	HCT 116	40.55 ± 0.59	42.67 ± 6.50	46.16[c]
	HT-29	44.25 ± 13.18	29.28 ± 7.84	48.59 ± 5.77
Pancreas	PANC-1	> 50	> 50	0.55 ± 0.07
Ovary	A2780	21.43 ± 2.08	17.57 ± 0.39	35.85 ± 21.58
Breast	MCF7	> 50	> 50	> 50
	MDA-MB-231	40.71 ± 3.33	34.21 ± 8.73	29.91 ± 2.26
	MDA-MB-453	23.32 ± 9.96	17.45 ± 0.64	43.06 ± 4.78
	T-47D	16.18[c]	17.92[c]	15.05[c]
Lung	WI-38 (normal)	48.05 ± 13.32	35.03 ± 3.84	> 50

[a] GI_{50} values were determined in-house by 72-h cell viability assays using MTT (adherent cell lines) or resazurin (suspension cell lines), and are presented as mean ± standard deviation derived from at least two replicates (unless otherwise stated). [b] ND: GI_{50} values were *not d*etermined. [c] GI_{50} values were acquired without replication.

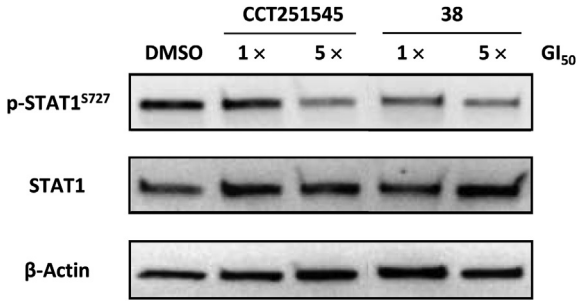

Fig. 5. Western blot analysis of MV4-11 cells incubated with **38** or CCT251545 for 2 h. DMSO diluent was used as a negative control, and β-actin antibody as an internal loading control. Both compounds were tested at the concentrations of their respective 1 × and 5 × GI_{50} values.

weakly by **39** (IC_{50} = 16.6 μM). These data showed a low potential for both compounds to induce CYP450-mediated drug-drug interactions if co-administered with other therapeutic agents. Cardiovascular toxicity remains one of the main reasons for post-approval withdrawal of drugs [58]. To understand the potential cardiotoxicity of **38** and **39**, their impacts on the human ether-à-go-go related gene (hERG) potassium channel were investigated. Both compounds had little inhibition on this cardiac ion channel, implying a slim likelihood of causing cardiotoxicity *in vivo*.

2.8. In Vivo Pharmacokinetic Properties of 38

Pharmacokinetic studies carried out in animals are at the heart of drug discovery programmes by virtue of their value of predicting

Table 7
In vitro drug-like properties of **38** and **39**.

Parameter[a]		**38**	39
Distribution coefficient: Log $D_{7.4}$[b]		4.21	> 4
Negative log of the acid dissociation constant: pKa[c]		4.90 ± 0.02	ND[h]
Aqueous solubility (μM)[d]		10-30	< 20
Caco-2 permeability[e]	A—B P_{app} (× 10^{-6} cm/s)	22.9 ± 0.6	20.4 ± 0.9
	B—A P_{app} (× 10^{-6} cm/s)	23.4 ± 3.2	19.5 ± 0.3
	Efflux ratio	1.02	0.96
Cytochrome P450 inhibition, IC_{50} (μM)[f]	CYP1A	7.7 ± 1.6	16.6 ± 1.8
	CYP2C9	> 25	> 25
	CYP2C19	> 25	> 25
	CYP2D6	> 25	> 25
	CYP3A4	4.59 ± 0.91	2.11 ± 0.21
hERG potassium channel inhibition, IC_{50} (μM)[g]		10.9 ± 2.2	14.7 ± 1.4

[a] All the data were acquired at Cyprotex Discovery Ltd.
[b] Using the shake flask assay with a buffer at pH 7.4.
sing a fas[c] Using a fast ultraviolet (UV) spectrometric titration.
[d] By turbidimetry.
[e] Using Caco-2 cell line that was derived from a human colon carcinoma and that resembles intestinal epithelial cells. Transport of a compound across the cell monolayer occurs in both directions: apical to basolateral (A—B) and basolateral to apical (B—A). P_{app}: apparent permeability coefficient; efflux ratio = P_{app}(B—A)/P_{app}(A—B).
[f] Using human liver microsomes in the presence of a CYP450 isoform-specific probe substrate: ethoxyresorufin for CYP1A, tolbutamide for CYP2C9, (*S*)-mephenytoin for CYP2C19, dextromethorphan for CYP2D6, and midazolam for CYP3A4. Typically, potent inhibition: IC_{50} < 1 μM; moderate inhibition: IC_{50} = 1–10 μM; weak or no inhibition: IC_{50} > 10 μM.
[g] Using CHO-hERG cells. Typically, highly potent inhibition: IC_{50} < 0.1 μM; potent inhibition: IC_{50} = 0.1–1 μM; moderate inhibition: IC_{50} = 1–10 μM; weak or no inhibition: IC_{50} > 10 μM.
[h] ND: pKa was *not d*etermined for **39**.

Table 8
In vivo pharmacokinetic properties of **38** in rats and mice.

Parameter[a]	CCT251545		**38**			
Species	Rat		Rat		Mouse	
Route	IV	PO	IV	PO	IV	PO
Dose (mg/kg)	5	20	5	20	2	10
C_{max} (μM)	10.6	4.06	14.4	2.77	3.44	5.01
T_{max} (h)	0.07	1.33	0.04	2.75	0.04	0.42
$T_{1/2}$ (h)	1.08	4.24	0.9	2.24	0.34	1.11
AUC (μM·h)	10.5	17.5	9.7	14.6	1.39	2.30
V_{dss} (L/kg)	1.38	–	1.11	–	1.99	–
Cl (L/h·kg)	1.20	–	1.39	–	3.78	–
F (%)	–	41	–	38	–	33

[a] Non-compartmental pharmacokinetic analysis was performed using Phoenix WinNonlin (Certara, St. Louis, MO, USA) for each curve of plasma concentration versus time, and mean values derived from three-to-four rats or ten mice are presented.

the pharmacokinetics, efficacy and safety of drugs in humans [59]. Inspired by the *in vitro* drug metabolism and pharmacokinetics (DMPK) profile of **38** (Table 7), single-dose pharmacokinetic studies were performed with male Sprague Dawley rats by an intravenous (IV) injection at 5 mg/kg or *per os* (PO) at 20 mg/kg, as well as with male BALB/c mice administered intravenously at 2 mg/kg or *via* oral gavage at 10 mg/kg (Table 8). For the sake of comparison, CCT251545 was also given to the same rat species using the identical dosages and routes of administration to those of **38**. Following the IV administration of **38**, volumes of distribution at steady state (V_{dss}) for rats (1.11 L/kg) and mice (1.99 L/kg) were much larger than total blood volumes of the respective murine species [60], indicating an extravascular distribution in both rodents. Plasma clearance (Cl) rates in rats and mice were found to be 1.39 and 3.78 L/h·kg, respectively; both values were not high relative to hepatic blood flow rates of the corresponding rodent species [60]. In parallel, after oral dosing of **38**, maximal plasma concentrations (C_{max}) of 2.77 μM in rats and 5.01 μM in mice were reached at 2.75 and 0.42 h, respectively, while values of half-life ($T_{1/2}$) were calculated to be 2.24 h in rats and 1.11 h in mice. The oral bioavailability (*F*) of **38** was 38% in rats and 33% in mice, achieving an *a*rea *u*nder the plasma concentration versus time *c*urve (AUC) value of 14.6 and 2.30 μM·h, respectively. In comparison with **38**, administration of CCT251545 to rats gave rise to a higher V_{dss} (1.38 L/kg) and a lower Cl (1.20 L/h·kg) in the IV route, but a larger AUC (17.5 μM·h) in the PO method, yielding a marginally higher *F* (41%).

2.9. In Vivo Toxicity of 38

We were aware of a report on severe systemic toxic effects of CCT251921, a potent CDK8 inhibitor that is structurally analogous to CCT251545 [51,52]. The observed toxicity was regarded as on-target effects [52], which has been challenged recently, with an argument that several off-target kinases could be responsible for the systemic toxicity of CCT251921 [61]. Accordingly, it was deemed advisable to conduct an initial assessment of the *in vivo* toxicity of **38**. Female BALB/c mice were orally administered **38** (70 mg/kg), CCT251545 (70 mg/kg), or vehicle (*i.e.*, 1% carboxymethyl cellulose (CMC) aqueous solution, 10 mL/kg) once daily for seven consecutive days, and observed for a further seven days. Individual body weights were recorded daily, showing little changes in mice treated with either **38** or vehicle and a rise of approximately 12% in the mouse following the seven-day administration of CCT251545 (Fig. S2). On day 15, all the mice were humanely killed prior to a collection of organs and tissues for histopathological examination or fluorescence-activated cell sorting (FACS) analysis.

Histopathological examination of long bones (left femora), lungs, hearts, livers, kidneys, intestines, uteri, ovaries and brains revealed pathological changes in the first two types of organs only after the treatment with **38** or CCT251545 (Fig. 6). The growth plate of the left femur collected from the CCT251545-treated mouse showed necrosis of chondrocytes, abnormal orientation of chondrocyte columns, and loss of ground substance, all of which led to extensive splitting of the cartilage (top panels in Fig. 6). Only mildly reduced ground substance and a few sightly disordered chondrocyte columns were found in **38**-treated mice. No morphological changes were apparent in the vehicle-dosed group. Interstitial pneumonitis was observed in the lungs of the mouse treated with CCT251545, with an increased number of alveolar macrophages detected (bottom panels in Fig. 6). In addition, vasculitis was developed in some of blood vessels, evidenced by infiltration of inflammatory cells and destruction of vessel walls. These lesions were much less severe in **38**-treated mice, whereas morphological changes in the vehicle-dosed group were very mild and were likely incidental to inhalation of the anaesthetic gas. Collectively, with the same dosage, **38** caused far less severe pathological alterations in left femora and lungs of mice than did CCT251545.

FACS analysis of splenocytes showed that no obvious changes in the percentages of dead cells, B cells, dendritic cells, granulocytes, monocytes/macrophages and neutrophils were detected when

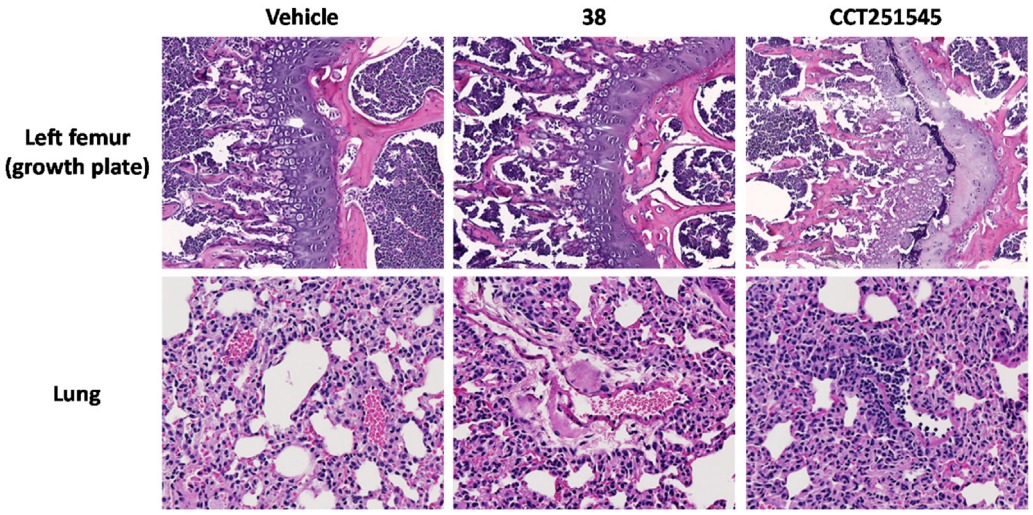

Fig. 6. Pathological changes to growth plates of left femora and lungs in mice after the treatment of vehicle (1% CMC, 10 mL/kg), **38** (70 mg/kg), or CCT251545 (70 mg/kg).

either drug-treated group was compared to the vehicle-dosed group, and that a slight increase in the percentage of CD3 T cells was observed in the CCT251545-treated mouse in comparison with vehicle-dosed mice (Fig. S3). Flow cytometric assessment of bone marrows revealed that there were no apparent differences in the percentages of dead cells, B cells and CD3 T cells among three treatment groups (Fig. S4). Overall, the treatment of **38** elicited little changes in immune cell subpopulations.

3. Conclusions

Capitalising on our in-house virtual screening results and the external discovery of CCT251545, a series of new multi-substituted pyridines was chemically synthesised and biologically evaluated. A close analysis of the structure-activity relationship of these compounds disclosed multiple potent CDK8 inhibitors, with **38** and **39** topping the rest. Their capability of inhibiting the kinase activity of cellular CDK8 was exemplified by the use of **38** in MV4-11 AML cells. While **38** and **39** displayed the selectivity for CDK8 in a screening against a panel of 62 kinases, both compounds exerted their potent anti-proliferative effects selectively on MV4-11 cell line. *In vivo* pharmacokinetic and toxicity studies demonstrated that **38** was not only orally bioavailable in rodents but also non-toxic towards the majority of murine organs and tissues.

4. Experimental

4.1. Chemistry

General synthetic procedure A

To a suspension of a bromide (1.00 equiv.), a boronic acid or a boronate ester (1.05–1.50 equiv.) and Pd(dppf)$Cl_2 \cdot CH_2Cl_2$ (0.05 equiv.) in CH_3CN (150 mM in bromide) was added 0.5 M aqueous Na_2CO_3 solution (1.40 equiv.). The reaction mixture was heated under microwave irradiation at 120–140 °C for 1 h, cooled down, diluted with distilled H_2O, and extracted with DCM (3 ×). The organic extracts were combined, washed with distilled H_2O (1 ×), and concentrated under reduced pressure. The residue was purified by Biotage® FlashMaster Personal$^+$ flash chromatography (and, when necessary, triturated or crystallised) to give the desired 5-substituted pyridine.

General synthetic procedure B

To a solution of a carboxylic acid (1.00 equiv.) in anhydrous DMF (100 mM in carboxylic acid) on an ice-salt bath were added DIPEA (3.00 equiv.) and HATU (1.10 equiv.). The reaction mixture was stirred for 10 min, and an amine (5.00 equiv.) added. The reaction mixture was warmed up to room temperature, stirred overnight, and diluted with distilled H_2O. The precipitate was collected by centrifugation, purified by Biotage® FlashMaster Personal$^+$ flash chromatography, and triturated or crystallised to give the desired amide.

General synthetic procedure C

To a suspension of LiOH (5.00 equiv.) in THF/CH_3OH (1:1, 250 mM in LiOH) was added a phenylsulfonyl-protected compound (1.00 equiv.). The reaction mixture was heated at 50 °C for 1 h, cooled down, diluted with distilled H_2O, and extracted with DCM (2 ×). The organic extracts were combined and concentrated under reduced pressure, and the residue was purified by Biotage® FlashMaster Personal$^+$ flash chromatography to give the desired unprotected form.

3-Bromo-4,5-dichloropyridine (2)

To a solution of LDA (2.0 M in THF/heptane/ethylbenzene, 6.25 mL, 12.5 mmol) in anhydrous THF (30 mL) at −78 °C was added a solution of 3-bromo-5-chloropyridine (**1**, 962 mg, 5.00 mmol) in anhydrous THF (10 mL). The reaction mixture was stirred for 1 h, and a solution of hexachloroethane (2.37 g, 10.0 mmol) in anhydrous THF (10 mL) added. The reaction mixture was stirred for 1 h, warmed up to room temperature, quenched with saturated aqueous NH_4Cl solution (30 mL), and extracted with DCM (3 × 100 mL). The organic extracts were combined and concentrated under reduced pressure, and the residue was purified by Biotage® FlashMaster Personal$^+$ flash chromatography (petroleum benzine ramping to petroleum benzine:DCM = 1:1) to give **2** as a yellow solid (735 mg, 65%). R_F (DCM:petroleum benzine = 1:4) 0.27. ^{1}H NMR ($CDCl_3$) δ 8.53 (s, 1H, pyridinyl-H), 8.62 (s, 1H, pyridinyl-H). ^{13}C NMR ($CDCl_3$) δ 122.1, 131.8, 142.5, 148.5, 150.5.

Methyl 1-(3-bromo-5-chloropyridin-4-yl)-1*H*-pyrrole-3-carboxylate (3)

To a solution of chloride **2** (227 mg, 1.00 mmol) and methyl 1*H*-pyrrole-3-carboxylate (126 mg, 1.01 mmol) in 1,4-dioxane (10 mL) was added Cs_2CO_3 (652 mg, 2.00 mmol). The reaction mixture was heated under microwave irradiation at 200 °C for 1 h, cooled down, diluted with distilled H_2O (30 mL), and extracted with DCM (3 × 30 mL). The organic extracts were combined and concentrated under reduced pressure, and the residue was purified by Biotage® FlashMaster Personal$^+$ flash chromatography (petroleum benzine ramping to petroleum benzine:EtOAc = 85:15) to give **3** as a white solid (152 mg, 48%). R_F (EtOAc:petroleum benzine = 1:4) 0.41. ^{1}H NMR ($CDCl_3$) δ 3.85 (s, 3H, CH_3), 6.69 (app t, 1H, *J* 3.0, pyrrolyl-H), 6.82 (dd, 1H, *J* 3.0 & 1.5, pyrrolyl-H), 7.37 (app t, 1H, *J* 1.5, pyrrolyl-H), 8.68 (s, 1H, pyridinyl-H), 8.78 (s, 1H, pyridinyl-H). ^{13}C NMR ($CDCl_3$) δ 51.5, 111.6, 118.5, 120.5, 122.4, 126.4, 130.6, 144.1, 149.7, 151.6, 164.7. HRMS (ESI+) 314.9540, 316.9519 & 318.9489 $[M+H]^+$; calcd. for $C_{11}H_9BrClN_2O_2^+$ 314.9531, 316.9510 & 318.9481 $[M+H]^+$.

4-(4-Chlorophenyl)-1-methyl-1*H*-pyrazole (5)

To a suspension of 1-chloro-4-iodobenzene (**4**, 7.16 g, 30.0 mmol) and 1-methyl-4-(4,4,5,5-tetramethyl-1,3,2-dioxaborolan-2-yl)-1*H*-pyrazole (6.25 g, 30.0 mmol) in THF/H_2O (98 mL/33 mL) were added Na_2CO_3 (7.00 g, 66.0 mmol) and Pd(dppf)$Cl_2 \cdot CH_2Cl_2$ (2.45 g, 3.00 mmol). The reaction mixture was heated at 80 °C overnight, cooled down and concentrated under reduced pressure. The residue was purified by flash column chromatography (petroleum benzine ramping to petroleum benzine:EtOAc = 1:1), and crystallised with DCM/*n*-hexane to give **5** as a brown solid (3.37 g, 58%). R_F (EtOAc:-petroleum benzine = 1:1) 0.33. ^{1}H NMR ($CDCl_3$) δ 3.93 (s, 3H, CH_3), 7.30 (d, 2H, *J* 8.5, 2 × phenyl-H), 7.37 (d, 2H, *J* 8.5, 2 × phenyl-H), 7.57 (s, 1H, pyrazolyl-H), 7.72 (s, 1H, pyrazolyl-H). ^{13}C NMR ($CDCl_3$) δ 39.2, 122.3, 126.8, 127.1, 129.1, 131.2, 132.0, 136.8 (two carbon signals overlapping or obscured). HRMS (ESI+) 193.0528 $[M(^{35}Cl)+H]^+$ & 195.0498 $[M(^{37}Cl)+H]^+$; calcd. for $C_{10}H_{10}ClN_2^+$ 193.0528 $[M(^{35}Cl)+H]^+$ & 195.0498 $[M(^{37}Cl)+H]^+$.

1-Methyl-4-(4-(4,4,5,5-tetramethyl-1,3,2-dioxaborolan-2-yl) phenyl)-1*H*-pyrazole (6)

To a suspension of chloride **5** (3.37 g, 17.5 mmol) and 4,4,4′,4′,5,5,5′,5′-octamethyl-2,2′-bi(1,3,2-dioxaborolane) (5.33 g, 21.0 mmol) in 1,4-dioxane (35 mL) were added AcOK (5.15 g, 52.5 mmol), $Pd_2(dba)_3$ (320 mg, 350 μmol) and XPhos (667 mg, 1.40 mmol). The reaction mixture was heated at 85 °C overnight, cooled down, and partitioned between distilled H_2O (250 mL) and EtOAc (250 mL). The mixture was filtered through a pad of Celite®, and the solids were washed with EtOAc (100 mL). The filtrate and washing were combined, and the organic layer was separated. The aqueous layer was extracted with EtOAc (2 × 100 mL). The organic layer and extracts were combined, dried over Na_2SO_4, and concentrated under reduced pressure. The residue was purified by Biotage® FlashMaster Personal$^+$ flash chromatography (DCM ramping to DCM:EtOAc = 9:1) to give **6** as a white solid (4.14 g, 83%). R_F (EtOAc:petroleum benzine = 1:1) 0.50. ^{1}H NMR ($CDCl_3$) δ 1.35 (s, 12H, 4 × dioxaborolanyl-CH_3), 3.94 (s, 3H, NCH_3), 7.47 (d,

2H, *J* 8.5, 2 × phenyl-H), 7.65 (s, 1H, pyrazolyl-H), 7.79 (d, 2H, *J* 8.0, 2 × phenyl-H), 7.80 (s, 1H, pyrazolyl-H). ^{13}C NMR ($CDCl_3$) δ 25.0, 39.2, 83.9, 123.2, 124.8, 127.4, 135.5, 135.6, 137.1 (seven carbon signals overlapping or obscured). HRMS (ESI+) 285.1772 $[M+H]^+$; calcd. for $C_{16}H_{22}BN_2O_2^+$ 285.1769 $[M+H]^+$.

Methyl 1-(3-chloro-5-(4-(1-methyl-1*H*-pyrazol-4-yl)phenyl) pyridin-4-yl)-1*H*-pyrrole-3-carboxylate (7)

Bromide **3** (140 mg, 444 μmol) and boronate ester **6** (133 mg, 468 μmol) were reacted at 120 °C using general synthetic procedure A. The residue was purified by Biotage® FlashMaster Personal$^+$ flash chromatography (DCM ramping to DCM:EtOAc = 7:3) to give **7** as a yellowish glue (117 mg, 67%). R_F (DCM:EtOAc = 3:2) 0.28. ^{1}H NMR ($CDCl_3$) δ 3.76 (s, 3H), 3.91 (s, 3H) (total 6H, 2 × CH_3), 6.47 (app t, 1H, *J* 2.0, pyrrolyl-H), 6.61 (dd, 1H, *J* 2.5 & 1.0, pyrrolyl-H), 7.02 (d, 2H, *J* 8.0, 2 × phenyl-H), 7.28 (app t, 1H, *J* 1.5, pyrrolyl-H), 7.38 (d, 2H, *J* 8.0, 2 × phenyl-H), 7.59 (s, 1H, pyrazolyl-H), 7.73 (s, 1H, pyrazolyl-H), 8.63 (s, 1H, pyridinyl-H), 8.71 (s, 1H, pyridinyl-H). ^{13}C NMR ($CDCl_3$) δ 39.2, 51.3, 111.2, 118.0, 122.2, 123.2, 125.9, 127.0, 127.2, 128.6, 129.0, 131.1, 133.3, 135.4, 136.9, 142.0, 149.6, 150.0, 164.8 (two carbon signals overlapping or obscured). HRMS (ESI+) 393.1112 $[M(^{35}Cl)+H]^+$ & 395.1085 $[M(^{37}Cl)+H]^+$; calcd. for $C_{21}H_{18}ClN_4O_2^+$ 393.1113 $[M(^{35}Cl)+H]^+$ & 395.1084 $[M(^{37}Cl)+H]^+$.

1-(3-Chloro-5-(4-(1-methyl-1*H*-pyrazol-4-yl)phenyl)pyridin-4-yl)-1*H*-pyrrole-3-carboxylic acid (8)

To a solution of ester **7** (110 mg, 280 μmol) in CH_3OH (2.8 mL) was added 1 M aqueous NaOH solution (2.80 mL, 2.80 mmol). The reaction mixture was heated at reflux for 2 h, cooled down, diluted with distilled H_2O (30 mL), washed with EtOAc (15 mL), taken to pH 2 with 2 M aqueous HCl solution, and extracted with DCM (3 × 15 mL). The organic extracts were combined and concentrated under reduced pressure, and the residue was purified by Biotage® FlashMaster Personal$^+$ flash chromatography (DCM ramping to DCM:CH_3OH = 91:9) to give **8** as a white solid (101 mg, 95%). R_F (DCM:CH_3OH = 94:6) 0.27. m.p. 253–254 °C. ^{1}H NMR (DMSO-d_6) δ 3.84 (s, 3H, CH_3), 6.46 (dd, 1H, *J* 2.5 & 1.5, pyrrolyl-H), 6.80 (app t, 1H, *J* 3.0, pyrrolyl-H), 7.14 (d, 2H, *J* 8.0, 2 × phenyl-H), 7.43 (app t, 1H, *J* 1.5, pyrrolyl-H), 7.53 (d, 2H, *J* 8.0, 2 × phenyl-H), 7.88 (s, 1H, pyrazolyl-H), 8.16 (s, 1H, pyrazolyl-H), 8.72 (s, 1H, pyridinyl-H), 8.85 (s, 1H, pyridinyl-H) (one carboxylic acid proton signal (COOH) not observed). ^{13}C NMR (DMSO-d_6) δ 38.8, 110.7, 118.0, 121.1, 123.9, 125.0, 127.5, 128.3, 128.8, 128.9, 130.9, 133.0, 135.5, 136.3, 142.0, 149.0, 149.9, 165.2 (two carbon signals overlapping or obscured). HRMS (ESI+) 379.0959 $[M(^{35}Cl)+H]^+$ & 381.0932 $[M(^{37}Cl)+H]^+$; calcd. for $C_{20}H_{16}ClN_4O_2^+$ 379.0957 $[M(^{35}Cl)+H]^+$ & 381.0927 $[M(^{37}Cl)+H]^+$. Anal. RP-HPLC Method A: t_R 16.13 min, purity >97%; Method B: t_R 9.60 min, purity >97%.

1-(3-Chloro-5-(4-(1-methyl-1*H*-pyrazol-4-yl)phenyl)pyridin-4-yl)-1*H*-pyrrole-3-carboxamide (9)

Carboxylic acid **8** (152 mg, 401 μmol) and NH_3 (0.5 M in 1,4-dioxane, 4.00 mL, 2.00 mmol) were coupled using general synthetic procedure B. The precipitate was collected by centrifugation, purified by Biotage® FlashMaster Personal$^+$ flash chromatography (DCM ramping to DCM:CH_3OH = 94:6), and triturated with *n*-hexane (3 mL) to give **9** as a white solid (111 mg, 73%). R_F (DCM:CH_3OH = 9:1) 0.47. m.p. 245–246 °C. ^{1}H NMR (DMSO-d_6) δ 3.84 (s, 3H, CH_3), 6.55 (dd, 1H, *J* 2.5 & 1.5, pyrrolyl-H), 6.74 (app t, 1H, *J* 2.5, pyrrolyl-H), 6.84 (br s, 1H, CON*H*H), 7.13 (d, 2H, *J* 8.0, 2 × phenyl-H), 7.32 (app t, 1H, *J* 1.5, pyrrolyl-H), 7.39 (br s, 1H, CONH*H*), 7.52 (d, 2H, *J* 8.0, 2 × phenyl-H), 7.88 (s, 1H, pyrazolyl-H), 8.16 (s, 1H, pyrazolyl-H), 8.72 (s, 1H, pyridinyl-H), 8.85 (s, 1H, pyridinyl-H). ^{13}C NMR (DMSO-d_6) δ 38.8, 109.6, 121.1, 121.6, 123.2, 124.9, 125.0, 128.3, 128.7, 128.8, 130.9, 132.9, 135.4, 136.3, 142.1, 149.0, 150.0, 165.1 (two carbon signals overlapping or obscured). HRMS (ESI+) 378.1125 $[M(^{35}Cl)+H]^+$ & 380.1099 $[M(^{37}Cl)+H]^+$; calcd. for $C_{20}H_{17}ClN_5O^+$ 378.1117 $[M(^{35}Cl)+H]^+$ & 380.1087 $[M(^{37}Cl)+H]^+$. Anal. RP-HPLC Method A: t_R 10.73 min, purity >98%; Method B: t_R 9.13 min, purity >99%.

1-(3-Chloro-5-(4-(1-methyl-1*H*-pyrazol-4-yl)phenyl)pyridin-4-yl)-*N*-methyl-1*H*-pyrrole-3-carboxamide (10)

Carboxylic acid **8** (152 mg, 401 μmol) and CH_3NH_2·HCl (136 mg, 2.01 mmol) were coupled using general synthetic procedure B. The precipitate was collected by centrifugation, purified by Biotage® FlashMaster Personal$^+$ flash chromatography (DCM ramping to DCM:EtOH = 94:6), and crystallised with DCM/*n*-hexane to give **10** as white crystals (110 mg, 70%). R_F (DCM:EtOH = 94:6) 0.39. m.p. 210–211 °C. ^{1}H NMR (DMSO-d_6) δ 2.66 (d, 3H, *J* 4.0, NHC*H*$_3$), 3.84 (s, 3H, pyrazolyl-CH_3), 6.54 (app s, 1H, pyrrolyl-H), 6.73 (app t, 1H, *J* 2.5, pyrrolyl-H), 7.13 (d, 2H, *J* 8.0, 2 × phenyl-H), 7.30 (app s, 1H, pyrrolyl-H), 7.52 (d, 2H, *J* 8.0, 2 × phenyl-H), 7.85 (q, 1H, *J* 4.5, N*H*CH$_3$), 7.88 (s, 1H, pyrazolyl-H), 8.16 (s, 1H, pyrazolyl-H), 8.72 (s, 1H, pyridinyl-H), 8.85 (s, 1H, pyridinyl-H). ^{13}C NMR (DMSO-d_6) δ 25.6, 38.8, 108.9, 121.1, 121.7, 123.2, 124.3, 125.0, 128.2, 128.7, 128.8, 130.9, 132.9, 135.3, 136.3, 142.1, 149.0, 150.0, 163.6 (two carbon signals overlapping or obscured). HRMS (ESI+) 392.1280 $[M(^{35}Cl)+H]^+$ & 394.1255 $[M(^{37}Cl)+H]^+$; calcd. for $C_{21}H_{19}ClN_5O^+$ 392.1273 $[M(^{35}Cl)+H]^+$ & 394.1244 $[M(^{37}Cl)+H]^+$. Anal. RP-HPLC Method A: t_R 10.93 min, purity >98%; Method B: t_R 9.40 min, purity >99%.

8-(3-Bromo-5-chloropyridin-4-yl)-2,8-diazaspiro[4.5]decan-1-one (11)

To a solution of chloride **2** (1.36 g, 5.99 mmol) and *tert*-butyl 1-oxo-2,8-diazaspiro[4.5]decane-8-carboxylate (1.83 g, 7.20 mmol) in 1-methoxy-2-propanol (10 mL) was added triethylamine (2.51 mL, 18.0 mmol). The reaction mixture was heated under microwave irradiation at 220 °C for 2.5 h, cooled down, diluted with DCM (40 mL), washed with distilled H_2O (2 × 20 mL), and concentrated under reduced pressure. The residue was purified by Biotage® FlashMaster Personal$^+$ flash chromatography (DCM ramping to DCM:EtOH = 96:4) to give **11** as a beige solid (1.63 g, 79%). R_F (DCM:EtOH = 96:4) 0.31. ^{1}H NMR ($CDCl_3$) δ 1.54 (d, 2H, *J* 13.0, CH_2), 2.08–2.16 (m, 2H, CH_2), 2.17 (t, 2H, *J* 7.0, CH_2), 3.30–3.44 (m, 4H, 2 × CH_2), 3.39 (t, 2H, *J* 7.0, CH_2), 5.90 (br s, 1H, CONH), 8.35 (s, 1H, pyridinyl-H), 8.49 (s, 1H, pyridinyl-H). ^{13}C NMR ($CDCl_3$) δ 31.5, 32.6, 39.0, 42.1, 47.0, 119.8, 129.2, 149.8, 151.6, 153.2, 182.1 (two carbon signals overlapping or obscured). HRMS (ESI+) 344.0167, 346.0149 & 348.0118 $[M+H]^+$; calcd. for $C_{13}H_{16}BrClN_3O^+$ 344.0160, 346.0140 & 348.0110 $[M+H]^+$.

8-(3-Chloro-5-(4-(1-methyl-1*H*-pyrazol-4-yl)phenyl)pyridin-4-yl)-2,8-diazaspiro[4.5]decan-1-one (CCT251545)

Bromide **11** (345 mg, 1.00 mmol) and boronate ester **6** (299 mg, 1.05 mmol) were reacted at 120 °C using general synthetic procedure A. The residue was purified by Biotage® FlashMaster Personal$^+$ flash chromatography (DCM ramping to DCM:CH_3OH = 96:4), and triturated with EtOAc (3 mL) to give CCT251545 as a white solid (300 mg, 71%). R_F (DCM:CH_3OH = 96:4) 0.20. m.p. 216–217 °C. ^{1}H NMR ($CDCl_3$) δ 1.35 (app d, 2H, *J* 13.0, CH_2), 1.94–1.99 (m, 2H, CH_2), 1.97 (t, 2H, *J* 6.5, CH_2), 2.74 (t, 2H, *J* 11.0, CH_2), 3.16 (dt, 2H, *J* 13.0 & 4.0, CH_2), 3.28 (t, 2H, *J* 6.5, CH_2), 3.96 (s, 3H, CH_3), 5.96 (br s, 1H, CONH), 7.28 (d, 2H, *J* 8.0, 2 × phenyl-H), 7.56 (d, 2H, *J* 8.0, 2 × phenyl-H), 7.68 (s, 1H, pyrazolyl-H), 7.82 (s, 1H, pyrazolyl-H), 8.21 (s, 1H, pyridinyl-H), 8.43 (s, 1H, pyridinyl-H). ^{13}C NMR ($CDCl_3$) δ 31.7, 32.4, 38.7, 39.3, 41.8, 47.8, 122.7, 125.6, 127.2, 128.3, 129.8, 132.3, 133.7, 135.7, 136.9, 149.6, 150.9, 152.9, 181.7 (four carbon signals overlapping or obscured). HRMS (ESI+) 422.1750 $[M(^{35}Cl)+H]^+$ & 424.1724 $[M(^{37}Cl)+H]^+$; calcd. for $C_{23}H_{25}ClN_5O^+$ 422.1742 $[M(^{35}Cl)+H]^+$ & 424.1713 $[M(^{37}Cl)+H]^+$. Anal. RP-HPLC Method A: t_R 14.55 min, purity >99%; Method B: t_R 8.41 min, purity >98%.

8-(3-Chloro-5-((1-methyl-1*H*-indazol-5-yl)amino)pyridin-4-yl)-2,8-diazaspiro[4.5]decan-1-one (12)

To a suspension of bromide **11** (345 mg, 1.00 mmol) and 1-

methyl-1*H*-indazol-5-amine (148 mg, 1.00 mmol) in 1,4-dioxane (10 mL) were added $Pd_2(dba)_3$ (45.8 mg, 50.0 μmol), Xantphos (28.9 mg, 50.1 μmol) and Cs_2CO_3 (652 mg, 2.00 mmol). The reaction mixture was heated under microwave irradiation at 180 °C for 1 h, cooled down, and partitioned between distilled H_2O (40 mL) and DCM (40 mL). The organic layer was separated, and the aqueous layer extracted with DCM (2 × 40 mL). The organic layer and extracts were combined and concentrated under reduced pressure, and the residue was purified by Biotage® FlashMaster Personal$^+$ flash chromatography (EtOAc ramping to EtOAc:CH_3OH = 96:4), and triturated with EtOAc/*n*-hexane (1 mL/2 mL) to give **12** as a beige solid (103 mg, 25%). R_F (EtOAc:CH_3OH = 95:5) 0.22. m.p. 203–204 °C. ^{1}H NMR ($CDCl_3$) δ 1.60 (app d, 2H, *J* 13.0, CH_2), 2.09 (td, 2H, *J* 12.5 & 4.0, CH_2), 2.22 (t, 2H, *J* 6.5, CH_2), 3.04 (app br s, 2H, CH_2), 3.40 (t, 2H, *J* 7.0, CH_2), 3.51 (app br s, 2H, CH_2), 4.09 (s, 3H, CH_3), 5.87 (br s, 1H), 6.84 (br s, 1H) (total 2H, CONH & pyridinyl-NH-indazolyl), 7.24 (dd, 1H, *J* 9.0 & 2.0, indazolyl-H), 7.39 (d, 1H, *J* 8.5, indazolyl-H), 7.53 (s, 1H, indazolyl-H), 7.92 (app s, 2H, indazolyl-H & pyridinyl-H), 8.20 (s, 1H, pyridinyl-H). ^{13}C NMR ($CDCl_3$) δ 31.1, 33.3, 35.9, 38.9, 42.0, 45.5, 110.2, 113.8, 124.0, 124.7, 129.8, 132.4, 133.6, 133.9, 137.8, 140.4, 140.6, 141.3, 181.7 (two carbon signals overlapping or obscured). HRMS (ESI+) 411.1697 [M(^{35}Cl)+H]$^+$ & 413.1680 [M(^{37}Cl)+H]$^+$; calcd. for $C_{21}H_{24}ClN_6O^+$ 411.1695 [M(^{35}Cl)+H]$^+$ & 413.1665 [M(^{37}Cl)+H]$^+$. Anal. RP-HPLC Method A: t_R 14.97 min, purity >98%; Method B: t_R 8.58 min, purity >98%.

1-Phenyl-4-(4,4,5,5-tetramethyl-1,3,2-dioxaborolan-2-yl)-1*H*-pyrazole

To a solution of 4-bromo-1-phenyl-1*H*-pyrazole (2.24 g, 10.0 mmol) and 4,4,4′,4′,5,5,5′,5′-octamethyl-2,2′-bi(1,3,2-dioxaborolane) (2.79 g, 11.0 mmol) in DMSO (25 mL) were added AcOK (2.95 g, 30.1 mmol) and Pd(dppf)Cl_2·CH_2Cl_2 (409 mg, 501 μmol). The reaction mixture was heated under N_2 at 80 °C for 20 h, cooled down, and partitioned between distilled H_2O (250 mL) and EtOAc (250 mL). The mixture was filtered through a pad of Celite®, and the solids were washed with EtOAc (250 mL). The filtrate and washing were combined, and the organic layer was separated. The aqueous layer was extracted with EtOAc (2 × 100 mL). The organic layer and extracts were combined, washed with distilled H_2O (2 × 100 mL) and brine (100 mL), and concentrated under reduced pressure. The residue was purified by Biotage® FlashMaster Personal$^+$ flash chromatography (DCM ramping to DCM:CH_3OH = 98:2) to give 1-phenyl-4-(4,4,5,5-tetramethyl-1,3,2-dioxaborolan-2-yl)-1*H*-pyrazole as a white solid (1.16 g, 43%). R_F (EtOAc:petroleum benzine = 1:9) 0.28. ^{1}H NMR ($CDCl_3$) δ 1.35 (s, 12H, 4 × CH_3), 7.30 (t, 1H, *J* 7.5, phenyl-H), 7.45 (t, 2H, *J* 8.0, 2 × phenyl-H), 7.70 (d, 2H, *J* 7.5, 2 × phenyl-H), 7.98 (s, 1H, pyrazolyl-H), 8.24 (s, 1H, pyrazolyl-H). ^{13}C NMR ($CDCl_3$) δ 25.0, 83.7, 119.6, 126.9, 129.6, 133.8, 140.0, 146.9 (seven carbon signals overlapping or obscured). HRMS (ESI+) 271.1621 [M+H]$^+$; calcd. for $C_{15}H_{20}BN_2O_2^+$ 271.1613 [M+H]$^+$.

8-(3-Chloro-5-(1-phenyl-1*H*-pyrazol-4-yl)pyridin-4-yl)-2,8-diazaspiro[4.5]decan-1-one (13)

Bromide **11** (173 mg, 502 μmol) and 1-phenyl-4-(4,4,5,5-tetramethyl-1,3,2-dioxaborolan-2-yl)-1*H*-pyrazole (149 mg, 552 μmol) were reacted at 120 °C using general synthetic procedure A. The residue was purified by Biotage® FlashMaster Personal$^+$ flash chromatography (DCM ramping to DCM:EtOH = 96.5:3.5), and washed with EtOAc (6 mL) to give **13** as a pinkish solid (90 mg, 44%). R_F (DCM:CH_3OH = 95:5) 0.34. m.p. 225–226 °C. ^{1}H NMR (DMSO-d_6) δ 1.35 (app d, 2H, *J* 12.5, CH_2), 1.75–1.88 (m, 2H, CH_2), 1.96 (t, 2H, *J* 7.0, CH_2), 2.95–3.12 (m, 4H, 2 × CH_2), 3.16 (t, 2H, *J* 7.0, CH_2), 7.34 (t, 1H, *J* 7.5, phenyl-H), 7.53 (t, 2H, *J* 7.5, phenyl-H), 7.57 (s, 1H, CONH), 7.93 (d, 2H, *J* 8.0, phenyl-H), 8.01 (s, 1H, pyrazolyl-H), 8.42 (s, 1H), 8.44 (s, 1H), 8.80 (s, 1H) (total 3H, pyrazolyl-H & 2 × pyridinyl-H). ^{13}C NMR (DMSO-d_6) δ 30.6, 31.8, 37.9, 41.3, 46.8, 118.4, 118.8, 125.9, 126.6, 126.8, 128.2, 129.7, 139.4, 141.1, 148.8, 150.3, 152.2, 180.1 (four carbon signals overlapping or obscured). HRMS (ESI+) 408.1586 [M(^{35}Cl)+H]$^+$ & 410.1558 [M(^{37}Cl)+H]$^+$; calcd. for $C_{22}H_{23}ClN_5O^+$ 408.1586 [M(^{35}Cl)+H]$^+$ & 410.1556 [M(^{37}Cl)+H]$^+$. Anal. RP-HPLC Method A: t_R 11.40 min, purity >97%; Method B: t_R 9.14 min, purity >99%.

8-(3-(1-Benzyl-1*H*-pyrazol-4-yl)-5-chloropyridin-4-yl)-2,8-diazaspiro[4.5]decan-1-one (14)

Bromide **11** (173 mg, 502 μmol) and 1-benzyl-4-(4,4,5,5-tetramethyl-1,3,2-dioxaborolan-2-yl)-1*H*-pyrazole (157 mg, 552 μmol) were reacted at 120 °C using general synthetic procedure A. The residue was purified by Biotage® FlashMaster Personal$^+$ flash chromatography (DCM ramping to DCM:CH_3OH = 96:4), triturated with *n*-hexane (3 mL), and washed with boiling EtOAc (5 mL) to give **14** as a beige solid (70 mg, 33%). R_F (DCM:CH_3OH = 95:5) 0.29. m.p. 167–168 °C. ^{1}H NMR (DMSO-d_6) δ 1.25 (app d, 2H, *J* 12.5, CH_2), 1.75 (td, 2H, *J* 12.0 & 4.0, CH_2), 1.82 (t, 2H, *J* 6.5, CH_2), 2.82 (t, 2H, *J* 10.5, CH_2), 2.94 (app d, 2H, *J* 12.5, CH_2), 3.14 (t, 2H, *J* 6.5, CH_2), 5.39 (s, 2H, phenyl-CH_2), 7.28–7.38 (m, 5H, 5 × phenyl-H), 7.57 (s, 1H, CONH), 7.70 (s, 1H, pyrazolyl-H), 8.07 (s, 1H, pyrazolyl-H), 8.30 (s, 1H, pyridinyl-H), 8.37 (s, 1H, pyridinyl-H). ^{13}C NMR (DMSO-d_6) δ 30.4, 31.8, 37.9, 41.3, 46.7, 55.0, 116.7, 126.5, 127.8, 128.2, 128.6, 130.1, 137.4, 138.8, 148.3, 150.4, 152.2, 180.1 (five carbon signals overlapping or obscured). HRMS (ESI+) 422.1742 [M(^{35}Cl)+H]$^+$ & 424.1719 [M(^{37}Cl)+H]$^+$; calcd. for $C_{23}H_{25}ClN_5O^+$ 422.1742 [M(^{35}Cl)+H]$^+$ & 424.1713 [M(^{37}Cl)+H]$^+$. Anal. RP-HPLC Method A: t_R 11.16 min, purity >95%; Method B: t_R 8.69 min, purity >98%.

8-(3-Chloro-5-(1-(tetrahydro-2*H*-pyran-4-yl)-1*H*-pyrazol-4-yl)pyridin-4-yl)-2,8-diazaspiro[4.5]decan-1-one (15)

Bromide **11** (173 mg, 502 μmol) and 1-(tetrahydro-2*H*-pyran-4-yl)-4-(4,4,5,5-tetramethyl-1,3,2-dioxaborolan-2-yl)-1*H*-pyrazole (167 mg, 600 μmol) were reacted at 135 °C using general synthetic procedure A. The residue was purified by Biotage® FlashMaster Personal$^+$ flash chromatography (DCM ramping to DCM:EtOH = 94:6) to give **15** as a beige solid (133 mg, 64%). R_F (DCM:EtOH = 94:6) 0.21. m.p. 215–216 °C. ^{1}H NMR (DMSO-d_6) δ 1.31 (app d, 2H, *J* 12.5, CH_2), 1.65–1.85 (m, 2H, CH_2), 1.94 (t, 2H, *J* 6.5, CH_2), 1.96–2.15 (m, 4H, 2 × CH_2), 2.96 (app br s, 4H, 2 × CH_2), 3.17 (t, 2H, *J* 6.5, CH_2), 3.49 (t, 2H, *J* 11.5, CH_2), 3.97 (d, 2H, *J* 10.5, CH_2), 4.35–4.55 (m, 1H, tetrahydropyranyl-CH), 7.56 (s, 1H), 7.72 (s, 1H), 8.10 (s, 1H), 8.34 (s, 1H), 8.36 (s, 1H) (total 5H, CONH & 2 × pyrazolyl-H & 2 × pyridinyl-H). ^{13}C NMR (DMSO-d_6) δ 30.6, 31.8, 32.9, 37.9, 41.2, 46.6, 57.4, 65.9, 115.9, 127.0, 127.6, 128.3, 138.0, 148.3, 150.1, 152.1, 180.1 (four carbon signals overlapping or obscured). HRMS (ESI+) 416.1855 [M(^{35}Cl)+H]$^+$ & 418.1813 [M(^{37}Cl)+H]$^+$; calcd. for $C_{21}H_{27}ClN_5O_2^+$ 416.1848 [M(^{35}Cl)+H]$^+$ & 418.1818 [M(^{37}Cl)+H]$^+$. Anal. RP-HPLC Method C: t_R 14.89 min, purity >99%; Method D: t_R 10.00 min, purity >99%.

***Tert*-butyl 4-(4-(5-chloro-4-(1-oxo-2,8-diazaspiro[4.5]decan-8-yl)pyridin-3-yl)-1*H*-pyrazol-1-yl)piperidine-1-carboxylate (16)**

Bromide **11** (173 mg, 502 μmol) and *tert*-butyl 4-(4-(4,4,5,5-tetramethyl-1,3,2-dioxaborolan-2-yl)-1*H*-pyrazol-1-yl)piperidine-1-carboxylate (208 mg, 551 μmol) were reacted at 120 °C using general synthetic procedure A. The residue was purified by Biotage® FlashMaster Personal$^+$ flash chromatography (DCM ramping to DCM:CH_3OH = 96:4), and crystallised with DCM/*n*-hexane to give **16** as a tan solid (80 mg, 31%). R_F (DCM:CH_3OH = 95:5) 0.29. m.p. 179–180 °C. ^{1}H NMR (DMSO-d_6) δ 1.30 (app d, 2H, *J* 13.0, CH_2), 1.41 (s, 9H, C(CH_3)$_3$), 1.66–1.88 (m, 4H, 2 × CH_2) 1.94 (t, 2H, *J* 6.5, CH_2), 2.08 (app d, 2H, *J* 11.0, CH_2), 2.70–3.06 (m, 6H, 3 × CH_2), 3.17 (t, 2H, *J* 6.5, CH_2), 4.04 (br d, 2H, *J* 9.5, CH_2), 4.36–4.46 (m, 1H, CH), 7.56 (s, 1H, CONH), 7.70 (s, 1H, pyrazolyl-H), 8.08 (s, 1H, pyrazolyl-H), 8.32 (s, 1H, pyridinyl-H), 8.36 (s, 1H, pyridinyl-H). ^{13}C NMR

(DMSO-d_6) δ 28.1, 30.6, 31.8, 32.0, 38.0, 41.3, 42.0, 42.7, 46.6, 58.3, 79.0, 116.0, 127.0, 127.7, 128.3, 138.1, 148.3, 150.1, 152.2, 153.9, 180.1 (five carbon signals overlapping or obscured). HRMS (ESI+) 515.2529 [M(^{35}Cl)+H]$^+$ & 517.2504 [M(^{37}Cl)+H]$^+$; calcd. for $C_{26}H_{36}ClN_6O_3^+$ 515.2532 [M(^{35}Cl)+H]$^+$ & 517.2502 [M(^{37}Cl)+H]$^+$. Anal. RP-HPLC Method A: t_R 11.58 min, purity >97%; Method B: t_R 9.31 min, purity >99%.

8-(3-Chloro-5-(1-methyl-1*H*-indazol-4-yl)pyridin-4-yl)-2,8-diazaspiro[4.5]decan-1-one (17)

Bromide **11** (173 mg, 502 μmol) and 1-methyl-4-(4,4,5,5-tetramethyl-1,3,2-dioxaborolan-2-yl)-1*H*-indazole (143 mg, 554 μmol) were reacted at 120 °C using general synthetic procedure A. The residue was purified by Biotage® FlashMaster Personal$^+$ flash chromatography (DCM ramping to DCM:CH_3OH = 96.5:3.5), triturated with *n*-hexane (5 mL), and washed with EtOAc (5 mL) to give **17** as a pinkish solid (76 mg, 38%). R_F (DCM:CH_3OH = 94:6) 0.37. m.p. 248–249 °C. ^{1}H NMR (DMSO-d_6) δ 1.12 (app d, 2H, *J* 12.5, CH_2), 1.59 (app t, 2H, *J* 10.5, CH_2), 1.64 (t, 2H, *J* 6.5, CH_2), 2.46 (t, 2H, *J* 12.0, CH_2), 2.90–3.10 (m, 2H, CH_2), 3.04 (t, 2H, *J* 6.5, CH_2), 4.10 (s, 3H, CH_3), 7.02 (d, 1H, *J* 6.5, indazolyl-H), 7.47 (s, 1H, CONH), 7.50 (t, 1H, *J* 7.5, indazolyl-H), 7.70 (d, 1H, *J* 8.5, indazolyl-H), 7.87 (s, 1H, indazolyl-H), 8.23 (s, 1H, pyridinyl-H), 8.51 (s, 1H, pyridinyl-H). ^{13}C NMR (DMSO-d_6) δ 30.3, 31.7, 35.6, 37.7, 41.2, 47.0, 109.5, 121.7, 123.1, 126.1, 127.1, 130.0, 130.6, 131.5, 139.7, 149.3, 150.6, 152.9, 179.8 (two carbon signals overlapping or obscured). HRMS (ESI+) 396.1590 [M(^{35}Cl)+H]$^+$ & 398.1560 [M(^{37}Cl)+H]$^+$; calcd. for $C_{21}H_{23}ClN_5O^+$ 396.1586 [M(^{35}Cl)+H]$^+$ & 398.1556 [M(^{37}Cl)+H]$^+$. Anal. RP-HPLC Method A: t_R 10.51 min, purity >98%; Method B: t_R 8.20 min, purity >99%.

8-(3-Chloro-5-(2-methyl-2*H*-indazol-4-yl)pyridin-4-yl)-2,8-diazaspiro[4.5]decan-1-one (18)

Bromide **11** (173 mg, 502 μmol) and 2-methyl-4-(4,4,5,5-tetramethyl-1,3,2-dioxaborolan-2-yl)-2*H*-indazole (143 mg, 553 μmol) were reacted at 120 °C using general synthetic procedure A. The residue was purified by Biotage® FlashMaster Personal$^+$ flash chromatography (DCM ramping to DCM:CH_3OH = 96:4), and triturated and washed with EtOAc (10 mL) to give **18** as a beige solid (80 mg, 40%). R_F (DCM:CH_3OH = 94:6) 0.36. m.p. 255–256 °C. ^{1}H NMR (DMSO-d_6) δ 1.12 (app d, 2H, *J* 12.5, CH_2), 1.59 (app t, 2H, *J* 10.0, CH_2), 1.66 (t, 2H, *J* 6.5, CH_2), 2.50–2.54 (m, 2H, CH_2), 2.90–3.10 (m, 2H, CH_2), 3.04 (t, 2H, *J* 6.5, CH_2), 4.14 (s, 3H, CH_3), 6.91 (d, 1H, *J* 7.0, indazolyl-H), 7.34 (t, 1H, *J* 8.0, indazolyl-H), 7.47 (s, 1H, CONH), 7.63 (d, 1H, *J* 8.5, indazolyl-H), 8.24 (s, 1H), 8.25 (s, 1H) (total 2H, indazolyl-H & pyridinyl-H), 8.49 (s, 1H, pyridinyl-H). ^{13}C NMR (DMSO-d_6) δ 30.4, 31.7, 37.8, 40.1, 41.2, 47.0, 116.6, 122.0, 122.1, 124.6, 125.4, 127.0, 129.6, 131.3, 148.1, 149.2, 150.4, 152.8, 179.9 (two carbon signals overlapping or obscured). HRMS (ESI+) 396.1587 [M(^{35}Cl)+H]$^+$ & 398.1559 [M(^{37}Cl)+H]$^+$; calcd. for $C_{21}H_{23}ClN_5O^+$ 396.1586 [M(^{35}Cl)+H]$^+$ & 398.1556 [M(^{37}Cl)+H]$^+$. Anal. RP-HPLC Method C: t_R 16.72 min, purity >98%; Method D: t_R 10.30 min, purity >99%.

8-(3-Chloro-5-(1*H*-indol-4-yl)pyridin-4-yl)-2,8-diazaspiro[4.5]decan-1-one (19)

Bromide **11** (173 mg, 502 μmol) and 4-(4,4,5,5-tetramethyl-1,3,2-dioxaborolan-2-yl)-1*H*-indole (134 mg, 551 μmol) were reacted at 120 °C using general synthetic procedure A. The residue was purified by Biotage® FlashMaster Personal$^+$ flash chromatography (DCM ramping to DCM:CH_3OH = 95:5), and crystallised with DCM/CH_3OH/EtOAc to give **19** as a pinkish solid (80 mg, 42%). R_F (DCM:CH_3OH = 94:6) 0.38. m.p. 296–297 °C. ^{1}H NMR (DMSO-d_6) δ 1.10 (app d, 2H, *J* 13.0, CH_2), 1.50–1.70 (m, 4H, 2 × CH_2), 2.30–2.50 (m, 2H, CH_2), 2.70–3.15 (m, 2H, CH_2), 3.03 (t, 2H, *J* 6.5, CH_2), 6.20 (app s, 1H, indolyl-H), 6.86 (d, 1H, *J* 7.0, indolyl-H), 7.19 (t, 1H, *J* 7.5, indolyl-H), 7.38 (app s, 1H, indolyl-H), 7.45 (d, 1H, *J* 7.0, indolyl-H), 7.46 (s, 1H, CONH), 8.19 (s, 1H, pyridinyl-H), 8.46 (s, 1H, pyridinyl-H), 11.28 (s, 1H, indolyl-NH). ^{13}C NMR (DMSO-d_6) δ 30.2, 31.7, 37.7, 41.3, 46.4, 100.0, 111.4, 120.4, 121.0, 126.1, 127.1, 127.2, 128.9, 132.2, 135.9, 148.6, 150.8, 153.1, 179.9 (two carbon signals overlapping or obscured). HRMS (ESI+) 381.1484 [M(^{35}Cl)+H]$^+$ & 383.1442 [M(^{37}Cl)+H]$^+$; calcd. for $C_{21}H_{22}ClN_4O^+$ 381.1477 [M(^{35}Cl)+H]$^+$ & 383.1447 [M(^{37}Cl)+H]$^+$. Anal. RP-HPLC Method C: t_R 14.57 min, purity >99%; Method D: t_R 10.54 min, purity >99%.

8-(3-Chloro-5-(isoquinolin-4-yl)pyridin-4-yl)-2,8-diazaspiro[4.5]decan-1-one (20)

Bromide **11** (173 mg, 502 μmol) and isoquinolin-4-ylboronic acid (95.5 mg, 552 μmol) were reacted at 120 °C using general synthetic procedure A. The residue was purified by Biotage® FlashMaster Personal$^+$ flash chromatography (DCM ramping to DCM:EtOH = 93:7), and crystallised with EtOAc/DCM to give **20** as a tan solid (70 mg, 36%). R_F (DCM:EtOH = 96:4) 0.14. m.p. 241–242 °C. ^{1}H NMR (DMSO-d_6) δ 1.03 (d, 2H, *J* 12.5, CH_2), 1.40–1.50 (m, 2H, CH_2), 1.49 (t, 2H, *J* 6.5, CH_2), 2.24 (t, 1H, *J* 11.0, C*H*H), 2.47 (t, 1H, *J* 11.0, CH*H*), 2.97 (t, 2H, *J* 6.5, CH_2), 2.97–3.07 (m, 2H, CH_2), 7.42 (s, 1H, CONH), 7.57 (d, 1H, *J* 8.0, isoquinolinyl-H), 7.75 (t, 1H, *J* 8.0, isoquinolinyl-H), 7.80 (t, 1H, *J* 8.0, isoquinolinyl-H), 8.23 (s, 1H), 8.24 (d, 1H, *J* 8.0), 8.44 (s, 1H), 8.59 (s, 1H), 9.40 (s, 1H) (total 5H, 3 × isoquinolinyl-H & 2 × pyridinyl-H). ^{13}C NMR (DMSO-d_6) δ 30.2, 31.6, 31.8, 37.7, 41.0, 46.5, 47.3, 124.3, 127.0, 127.8, 127.9, 128.0, 128.2, 128.4, 131.5, 134.1, 143.4, 150.1, 151.2, 152.8, 153.9, 179.7. HRMS (ESI+) 393.1476 [M(^{35}Cl)+H]$^+$ & 395.1446 [M(^{37}Cl)+H]$^+$; calcd. for $C_{22}H_{22}ClN_4O^+$ 393.1477 [M(^{35}Cl)+H]$^+$ & 395.1447 [M(^{37}Cl)+H]$^+$. Anal. RP-HPLC Method A: t_R 10.76 min, purity >97%; Method B: t_R 8.16 min, purity >99%.

8-(3-Chloro-5-(quinolin-4-yl)pyridin-4-yl)-2,8-diazaspiro[4.5]decan-1-one (21)

Bromide **11** (173 mg, 502 μmol) and quinolin-4-ylboronic acid (95.5 mg, 552 μmol) were reacted at 120 °C using general synthetic procedure A. The residue was purified by Biotage® FlashMaster Personal$^+$ flash chromatography (DCM ramping to DCM:CH_3OH = 95:5), and washed with EtOAc (5 mL) and *n*-hexane (3 mL) to give **21** as a beige solid (136 mg, 69%). R_F (DCM:CH_3OH = 94:6) 0.39. m.p. 218–219 °C. ^{1}H NMR (DMSO-d_6) δ 1.04 (dd, 2H, *J* 16.0 & 14.5, CH_2), 1.45 (td, 2H, *J* 12.5 & 2.5, CH_2), 1.51 (t, 2H, *J* 6.5, CH_2), 2.23 (t, 1H, *J* 11.0, C*H*H), 2.53 (t, 1H, *J* 11.0, CH*H*), 2.98 (t, 2H, *J* 6.5, CH_2), 2.98–3.08 (m, 2H, CH_2), 7.42 (s, 1H, CONH), 7.50 (d, 1H, *J* 4.0, quinolinyl-H), 7.55–7.66 (m, 2H, 2 × quinolinyl-H), 7.77–7.87 (m, 1H, quinolinyl-H), 8.12 (d, 1H, *J* 8.5, quinolinyl-H), 8.21 (s, 1H, pyridinyl-H), 8.60 (s, 1H, pyridinyl-H), 8.99 (d, 1H, *J* 4.5, quinolinyl-H). ^{13}C NMR (DMSO-d_6) δ 30.4, 31.6, 31.8, 37.8, 41.1, 46.5, 47.3, 122.8, 125.6, 126.8, 127.0, 127.5, 128.7, 129.6, 130.0, 143.7, 147.9, 150.3, 150.4, 150.6, 153.4, 179.8. HRMS (ESI+) 393.1476 [M(^{35}Cl)+H]$^+$ & 395.1451 [M(^{37}Cl)+H]$^+$; calcd. for $C_{22}H_{22}ClN_4O^+$ 393.1477 [M(^{35}Cl)+H]$^+$ & 395.1447 [M(^{37}Cl)+H]$^+$. Anal. RP-HPLC Method C: t_R 17.90 min, purity >98%; Method D: t_R 10.98 min, purity >99%.

8-(3-Chloro-5-(quinolin-5-yl)pyridin-4-yl)-2,8-diazaspiro[4.5]decan-1-one (22)

Bromide **11** (173 mg, 502 μmol) and quinolin-5-ylboronic acid (95.5 mg, 552 μmol) were reacted at 120 °C using general synthetic procedure A. The residue was purified by Biotage® FlashMaster Personal$^+$ flash chromatography (DCM ramping to DCM:CH_3OH = 94:6), and washed with EtOAc (5 mL) and *n*-hexane (3 mL) to give **22** as a beige solid (100 mg, 51%). R_F (DCM:CH_3OH = 94:6) 0.30. m.p. 195–196 °C. ^{1}H NMR (DMSO-d_6) δ 1.01 (t, 2H, *J* 12.0, CH_2), 1.30–1.50 (m, 2H, CH_2), 1.50 (t, 2H, *J* 6.5, CH_2), 2.24 (t, 1H, *J* 11.0, C*H*H), 2.38 (t, 1H, *J* 12.0, CH*H*), 2.92 (d, 1H, *J* 12.5, C*H*H), 2.97 (t, 2H, *J* 6.5, CH_2), 3.02 (d, 1H, *J* 12.5, CH*H*), 7.40 (s, 1H, CONH), 7.52 (dd, 1H, *J* 9.0 & 4.5, quinolinyl-H), 7.54 (d, 1H, *J* 7.0, quinolinyl-H), 7.87 (t, 1H, *J* 8.0, quinolinyl-H), 7.96 (d, 1H, *J* 8.5, quinolinyl-H), 8.10 (d, 1H, *J* 8.5, quinolinyl-H), 8.18 (s, 1H, pyridinyl-H), 8.56 (s, 1H, pyridinyl-H), 8.94 (dd, 1H, *J* 4.0 & 1.5, quinolinyl-H).

^{13}C NMR (DMSO-d_6) δ 30.4, 31.7, 31.9, 37.9, 41.2, 46.5, 47.3, 122.3, 126.9, 127.2, 128.7, 129.5, 129.6, 130.3, 134.1, 135.4, 147.8, 150.0, 151.0, 151.2, 153.9, 180.0. HRMS (ESI+) 393.1478 [M(^{35}Cl)+H]$^+$ & 395.1454 [M(^{37}Cl)+H]$^+$; calcd. for $C_{22}H_{22}ClN_4O^+$ 393.1477 [M(^{35}Cl)+H]$^+$ & 395.1447 [M(^{37}Cl)+H]$^+$. Anal. RP-HPLC Method C: t_R 17.08 min, purity >99%; Method D: t_R 10.09 min, purity >99%.

8-(3-Chloro-5-(isoquinolin-5-yl)pyridin-4-yl)-2,8-diazaspiro [4.5]decan-1-one (23)

Bromide **11** (173 mg, 502 μmol) and isoquinolin-5-ylboronic acid (95.5 mg, 552 μmol) were reacted at 120 °C using general synthetic procedure A. The residue was purified by Biotage® FlashMaster Personal$^+$ flash chromatography (DCM ramping to DCM:CH_3OH = 94:6), and washed with EtOAc (5 mL) and *n*-hexane (3 mL) to give **23** as a beige solid (45 mg, 23%). R_F (DCM:CH_3OH = 94:6) 0.30. m.p. 205–206 °C. ^{1}H NMR (DMSO-d_6) δ 1.02 (d, 2H, *J* 13.0, CH_2), 1.44 (t, 2H, *J* 12.0, CH_2), 1.50 (t, 2H, *J* 6.5, CH_2), 2.25 (t, 1H, *J* 12.0, C*H*H), 2.44 (t, 1H, *J* 12.0, CH*H*), 2.94 (d, 1H, *J* 13.0, C*H*H), 2.98 (t, 2H, *J* 6.5, CH_2), 3.02 (d, 1H, *J* 13.0, CH*H*), 7.40 (d, 1H, *J* 6.5, isoquinolinyl-H), 7.41 (s, 1H, CONH), 7.73 (d, 1H, *J* 7.0, isoquinolinyl-H), 7.80 (t, 1H, *J* 7.5, isoquinolinyl-H), 8.19 (s, 1H, pyridinyl-H), 8.23 (d, 1H, *J* 8.0, isoquinolinyl-H), 8.48 (d, 1H, *J* 6.0, isoquinolinyl-H), 8.58 (s, 1H, pyridinyl-H), 9.40 (s, 1H, isoquinolinyl-H). ^{13}C NMR (DMSO-d_6) δ 30.3, 31.6, 31.8, 37.7, 41.0, 46.4, 47.3, 118.1, 127.1, 127.4, 128.3, 130.0, 132.4, 133.9, 134.1, 143.7, 149.9, 151.1, 152.9, 153.8, 179.8 (one carbon signal overlapping or obscured). HRMS (ESI+) 393.1478 [M(^{35}Cl)+H]$^+$ & 395.1450 [M(^{37}Cl)+H]$^+$; calcd. for $C_{22}H_{22}ClN_4O^+$ 393.1477 [M(^{35}Cl)+H]$^+$ & 395.1447 [M(^{37}Cl)+H]$^+$. Anal. RP-HPLC Method C: t_R 15.94 min, purity >97%; Method D: t_R 9.25 min, purity >98%.

8-(3-Chloro-5-(isoquinolin-8-yl)pyridin-4-yl)-2,8-diazaspiro [4.5]decan-1-one (24)

Bromide **11** (173 mg, 502 μmol) and isoquinolin-8-ylboronic acid (95.5 mg, 552 μmol) were reacted at 120 °C using general synthetic procedure A. The residue was purified by Biotage® FlashMaster Personal$^+$ flash chromatography (DCM ramping to DCM:CH_3OH = 94:6), and washed with EtOAc (5 mL) and *n*-hexane (3 mL) to give **24** as a beige solid (110 mg, 56%). R_F (DCM:CH_3OH = 94:6) 0.34. m.p. 198–199 °C. ^{1}H NMR (DMSO-d_6) δ 1.00 (t, 2H, *J* 8.5, CH_2), 1.32–1.46 (m, 2H, CH_2), 1.48 (t, 2H, *J* 6.5, CH_2), 2.23 (t, 1H, *J* 11.0, C*H*H), 2.42 (t, 1H, *J* 11.0, CH*H*), 2.97 (t, 2H, *J* 6.5, CH_2), 2.97–3.15 (m, 2H, CH_2), 7.40 (s, 1H, CONH), 7.59 (d, 1H, *J* 6.5, isoquinolinyl-H), 7.88 (t, 1H, *J* 7.5, isoquinolinyl-H), 7.93 (d, 1H, *J* 5.5, isoquinolinyl-H), 8.07 (d, 1H, *J* 8.0, isoquinolinyl-H), 8.26 (s, 1H, pyridinyl-H), 8.56 (d, 1H, *J* 5.5, isoquinolinyl-H), 8.59 (s, 1H, pyridinyl-H), 8.89 (s, 1H, isoquinolinyl-H). ^{13}C NMR (DMSO-d_6) δ 30.3, 31.5, 31.8, 37.7, 41.0, 46.5, 47.2, 120.8, 126.5, 127.1, 127.3, 129.6, 129.9, 130.5, 135.2, 135.6, 143.2, 150.1, 150.2, 151.0, 153.7, 179.7. HRMS (ESI+) 393.1476 [M(^{35}Cl)+H]$^+$ & 395.1450 [M(^{37}Cl)+H]$^+$; calcd. for $C_{22}H_{22}ClN_4O^+$ 393.1477 [M(^{35}Cl)+H]$^+$ & 395.1447 [M(^{37}Cl)+H]$^+$. Anal. RP-HPLC Method C: t_R 15.97 min, purity >99%; Method D: t_R 9.53 min, purity >98%.

8-(3-Chloro-5-(quinolin-8-yl)pyridin-4-yl)-2,8-diazaspiro [4.5]decan-1-one (25)

Bromide **11** (173 mg, 502 μmol) and quinolin-8-ylboronic acid (95.5 mg, 552 μmol) were reacted at 120 °C using general synthetic procedure A. The residue was purified by Biotage® FlashMaster Personal$^+$ flash chromatography (DCM ramping to DCM:EtOH = 95.5:4.5), and crystallised with EtOAc/DCM to give **25** as a tan solid (60 mg, 30%). R_F (DCM:EtOH = 96:4) 0.30. m.p. 203–204 °C. ^{1}H NMR (DMSO-d_6) δ 1.00 (d, 1H, *J* 12.5, C*H*H), 1.05 (d, 1H, *J* 12.5, CH*H*), 1.35–1.52 (m, 3H, C*H*H & CH_2), 1.53 (t, 1H, *J* 9.5, CH*H*), 2.02 (t, 1H, *J* 10.0, C*H*H), 2.50–2.58 (m, 1H, CH*H*), 2.90 (d, 1H, *J* 12.0, C*H*H), 2.92–3.02 (m, 3H, CH*H* & CH_2), 7.42 (s, 1H, CONH), 7.59 (dd, 1H, *J* 8.0 & 4.5, quinolinyl-H), 7.72 (d, 2H, *J* 5.0, 2 × quinolinyl-H), 8.08 (t, 1H, *J* 4.5, 2 × quinolinyl-H), 8.16 (s, 1H, pyridinyl-H), 8.46 (d, 1H, *J* 8.0, quinolinyl-H), 8.49 (s, 1H, pyridinyl-H), 8.87 (d, 1H, *J* 2.5, quinolinyl-H). ^{13}C NMR (DMSO-d_6) δ 30.1, 31.5, 31.8, 37.6, 41.1, 46.0, 47.0, 121.8, 126.4, 126.8, 127.9, 128.8, 130.8, 131.0, 136.5, 136.6, 146.1, 148.8, 150.6, 151.3, 153.9, 179.7. HRMS (ESI+) 393.1477 [M(^{35}Cl)+H]$^+$ & 395.1450 [M(^{37}Cl)+H]$^+$; calcd. for $C_{22}H_{22}ClN_4O^+$ 393.1477 [M(^{35}Cl)+H]$^+$ & 395.1447 [M(^{37}Cl)+H]$^+$. Anal. RP-HPLC Method A: t_R 9.82 min, purity >97%; Method B: t_R 7.89 min, purity >99%.

8-(3-Chloro-5-(naphthalen-1-yl)pyridin-4-yl)-2,8-diazaspiro [4.5]decan-1-one (26)

Bromide **11** (173 mg, 502 μmol) and naphthalen-1-ylboronic acid (95.0 mg, 552 μmol) were reacted at 120 °C using general synthetic procedure A. The residue was purified by Biotage® FlashMaster Personal$^+$ flash chromatography (DCM ramping to DCM:EtOH = 97:3), triturated with *n*-hexane (5 mL), and washed with EtOAc (3 mL) to give **26** as a white solid (120 mg, 61%). R_F (DCM:CH_3OH = 96:4) 0.33. m.p. 203–204 °C. ^{1}H NMR (DMSO-d_6) δ 0.96–1.08 (m, 2H, CH_2), 1.46 (t, 2H, *J* 7.0, CH_2), 1.46–1.54 (m, 2H, CH_2), 2.17 (t, 1H, *J* 11.5, C*H*H), 2.40 (t, 1H, *J* 11.5, CH*H*), 2.85–3.05 (m, 2H, CH_2), 2.97 (t, 2H, *J* 7.0, CH_2), 7.35–7.47 (m, 2H), 7.47–7.54 (m, 2H), 7.54–7.59 (m, 1H) (total 5H, CONH & 4 × naphthalenyl-H), 7.62 (t, 1H, *J* 7.5, naphthalenyl-H), 8.02 (d, 2H, *J* 8.0, 2 × naphthalenyl-H), 8.18 (s, 1H, pyridinyl-H), 8.56 (s, 1H, pyridinyl-H). ^{13}C NMR (DMSO-d_6) δ 30.1, 31.6, 31.7, 37.6, 41.0, 46.1, 47.2, 125.3, 125.6, 126.3, 126.8, 127.0, 128.1, 128.4, 128.5, 131.2, 131.6, 133.1, 134.6, 149.4, 151.1, 153.7, 179.7. HRMS (ESI+) 392.1527 [M(^{35}Cl)+H]$^+$ & 394.1501 [M(^{37}Cl)+H]$^+$; calcd. for $C_{23}H_{23}ClN_3O^+$ 392.1524 [M(^{35}Cl)+H]$^+$ & 394.1495 [M(^{37}Cl)+H]$^+$. Anal. RP-HPLC Method A: t_R 9.28 min, purity >98%; Method B: t_R 11.84 min, purity >97%.

8-(3-Chloro-5-(4-methylnaphthalen-1-yl)pyridin-4-yl)-2,8-diazaspiro[4.5]decan-1-one (27)

Bromide **11** (173 mg, 502 μmol) and (4-methylnaphthalen-1-yl) boronic acid (103 mg, 554 μmol) were reacted at 120 °C using general synthetic procedure A. The residue was purified by Biotage® FlashMaster Personal$^+$ flash chromatography (DCM ramping to DCM:CH_3OH = 97.5:2.5), and triturated and washed with *n*-hexane (10 mL) to give **27** as a white solid (110 mg, 54%). R_F (DCM:CH_3OH = 94:6) 0.33. m.p. 195–196 °C. ^{1}H NMR (DMSO-d_6) δ 1.04 (app d, 2H, *J* 13.0, CH_2), 1.47 (t, 2H, *J* 6.5, CH_2), 1.50–1.60 (m, 2H, CH_2), 2.18 (t, 1H, *J* 12.0, C*H*H), 2.42 (t, 1H, *J* 12.0, CH*H*), 2.72 (s, 3H, CH_3), 2.92 (app d, 1H, *J* 13.0, C*H*H), 2.97 (t, 2H, *J* 6.5, CH_2), 3.02 (app d, 1H, *J* 12.5, CH*H*), 7.31 (d, 1H, *J* 7.0, naphthalenyl-H), 7.42 (s, 1H, CONH), 7.47 (d, 1H, *J* 7.0, naphthalenyl-H), 7.50–7.57 (m, 2H, 2 × naphthalenyl-H), 7.57–7.66 (m, 1H, naphthalenyl-H), 8.11 (d, 1H, *J* 8.5, naphthalenyl-H), 8.12 (s, 1H, pyridinyl-H), 8.54 (s, 1H, pyridinyl-H). ^{13}C NMR (DMSO-d_6) δ 19.3, 30.3, 31.7, 31.8, 37.7, 41.2, 46.2, 47.3, 124.8, 126.0, 126.3, 126.4, 126.5, 127.1, 127.9, 131.4, 131.8, 132.2, 133.0, 134.7, 149.3, 151.4, 153.8, 179.8. HRMS (ESI+) 406.1679 [M(^{35}Cl)+H]$^+$ & 408.1655 [M(^{37}Cl)+H]$^+$; calcd. for $C_{24}H_{25}ClN_3O^+$ 406.1681 [M(^{35}Cl)+H]$^+$ & 408.1651 [M(^{37}Cl)+H]$^+$. Anal. RP-HPLC Method C: t_R 21.36 min, purity >99%; Method D: t_R 14.02 min, purity >97%.

8-(3-Chloro-5-(4-methoxynaphthalen-1-yl)pyridin-4-yl)-2,8-diazaspiro[4.5]decan-1-one (28)

Bromide **11** (173 mg, 502 μmol) and 2-(4-methoxynaphthalen-1-yl)-4,4,5,5-tetramethyl-1,3,2-dioxaborolane (157 mg, 552 μmol) were reacted at 120 °C using general synthetic procedure A. The residue was purified by Biotage® FlashMaster Personal$^+$ flash chromatography (DCM ramping to DCM:CH_3OH = 97.5:2.5), and washed with EtOAc (3 mL) and *n*-hexane (3 mL) to give **28** as a white solid (120 mg, 57%). R_F (DCM:CH_3OH = 94:6) 0.41. m.p. 255–256 °C. ^{1}H NMR (DMSO-d_6) δ 1.04 (t, 2H, *J* 11.5, CH_2), 1.48 (t, 2H, *J* 6.5, CH_2), 1.50–1.62 (m, 2H, CH_2), 2.16 (t, 1H, *J* 11.5, C*H*H), 2.46 (t, 1H, *J* 11.5, CH*H*), 2.90–3.20 (m, 2H, CH_2), 2.98 (t, 2H, *J* 6.0, CH_2), 4.02 (s, 3H, CH_3), 7.08 (d, 1H, *J* 8.0, naphthalenyl-H), 7.35 (d, 1H, *J* 8.0, naphthalenyl-H), 7.42 (s, 1H, CONH), 7.45 (d, 1H, *J* 8.0, naphthalenyl-

H), 7.48–7.62 (m, 2H, 2 × naphthalenyl-H), 8.13 (s, 1H, pyridinyl-H), 8.24 (d, 1H, *J* 8.0, naphthalenyl-H), 8.52 (s, 1H, pyridinyl-H). ^{13}C NMR (DMSO-d_6) δ 30.2, 31.6, 31.8, 37.8, 41.2, 46.2, 47.2, 55.8, 104.2, 122.0, 124.8, 125.4, 125.7, 126.7, 127.0, 127.2, 128.5, 131.2, 132.6, 149.2, 151.6, 154.0, 155.0, 179.9. HRMS (ESI+) 422.1630 [M(^{35}Cl)+H]$^+$ & 424.1608 [M(^{37}Cl)+H]$^+$; calcd. for $C_{24}H_{25}ClN_3O_2^+$ 422.1630 [M(^{35}Cl)+H]$^+$ & 424.1600 [M(^{37}Cl)+H]$^+$. Anal. RP-HPLC Method C: t_R 20.85 min, purity >99%; Method D: t_R 13.43 min, purity >99%.

8-(3-Chloro-5-(dibenzo[*b*,*d*]furan-4-yl)pyridin-4-yl)-2,8-diazaspiro[4.5]decan-1-one (29)

Bromide **11** (173 mg, 502 μmol) and dibenzo[*b*,*d*]furan-4-ylboronic acid (117 mg, 552 μmol) were reacted at 120 °C using general synthetic procedure A. The residue was purified by Biotage® FlashMaster Personal$^+$ flash chromatography (DCM ramping to DCM:CH_3OH = 97.5:2.5) to give **29** as a beige solid (125 mg, 58%). R_F (DCM:CH_3OH = 94:6) 0.40. m.p. 215–216 °C. ^{1}H NMR (DMSO-d_6) δ 1.11 (app d, 2H, *J* 12.5, CH_2), 1.48 (t, 2H, *J* 6.5, CH_2), 1.59 (t, 2H, *J* 9.5, CH_2), 2.50–2.72 (m, 2H, CH_2), 2.96 (t, 2H, *J* 6.5, CH_2), 3.07 (d, 2H, *J* 11.5, CH_2), 7.40–7.47 (m, 2H), 7.47–7.57 (m, 3H) (total 5H, CONH & 4 × dibenzofuranyl-H), 7.68 (d, 1H, *J* 8.5, dibenzofuranyl-H), 8.22 (t, 2H, *J* 7.0, 2 × dibenzofuranyl-H), 8.34 (s, 1H, pyridinyl-H), 8.55 (s, 1H, pyridinyl-H). ^{13}C NMR (DMSO-d_6) δ 30.2, 31.8, 37.6, 41.0, 46.7, 111.7, 121.2, 121.5, 121.7, 123.4, 123.5, 123.6, 123.7, 126.9, 127.2, 128.0, 128.5, 149.6, 151.2, 152.9, 153.2, 155.5, 179.7 (two carbon signals overlapping or obscured). HRMS (ESI+) 432.1469 [M(^{35}Cl)+H]$^+$ & 434.1452 [M(^{37}Cl)+H]$^+$; calcd. for $C_{25}H_{23}ClN_3O_2^+$ 432.1473 [M(^{35}Cl)+H]$^+$ & 434.1444 [M(^{37}Cl)+H]$^+$. Anal. RP-HPLC Method C: t_R 20.74 min, purity >99%; Method D: t_R 15.14 min, purity >99%.

8-(3-Chloro-5-(dibenzo[*b*,*d*]thiophen-4-yl)pyridin-4-yl)-2,8-diazaspiro[4.5]decan-1-one (30)

Bromide **11** (173 mg, 502 μmol) and dibenzo[*b*,*d*]thiophen-4-ylboronic acid (126 mg, 552 μmol) were reacted at 120 °C using general synthetic procedure A. The residue was purified by Biotage® FlashMaster Personal$^+$ flash chromatography (DCM ramping to DCM:CH_3OH = 97.5:2.5) to give **30** as a white solid (100 mg, 44%). R_F (DCM:CH_3OH = 94:6) 0.41. m.p. 245–246 °C. ^{1}H NMR (DMSO-d_6) δ 1.13 (t, 2H, *J* 14.0, CH_2), 1.40–1.75 (m, 4H, 2 × CH_2), 2.50–2.65 (m, 2H, CH_2), 2.76–2.92 (m, 1H, C*H*H), 3.00 (t, 2H, *J* 6.5, CH_2), 3.10–3.40 (m, 1H, CH*H*), 7.37–7.49 (m, 2H), 7.49–7.60 (m, 2H) (total 4H, CONH & 3 × dibenzofuranyl-H), 7.66 (t, 1H, *J* 7.5, dibenzofuranyl-H), 8.00 (d, 1H, *J* 7.0, dibenzofuranyl-H), 8.31 (s, 1H, pyridinyl-H), 8.43 (t, 2H, *J* 8.0, dibenzofuranyl-H), 8.57 (s, 1H, pyridinyl-H). ^{13}C NMR (DMSO-d_6) δ 30.4, 31.6, 31.8, 37.7, 41.1, 46.4, 47.6, 121.9, 122.5, 123.2, 125.1, 125.3, 127.0, 127.5, 128.8, 131.1, 132.1, 135.3, 135.6, 138.4, 139.1, 150.0, 150.2, 153.1, 179.7. HRMS (ESI+) 448.1246 [M(^{35}Cl)+H]$^+$ & 450.1206 [M(^{37}Cl)+H]$^+$; calcd. for $C_{25}H_{23}ClN_3OS^+$ 448.1245 [M(^{35}Cl)+H]$^+$ & 450.1215 [M(^{37}Cl)+H]$^+$. Anal. RP-HPLC Method C: t_R 21.48 min, purity >99%; Method D: t_R 16.22 min, purity >99%.

8-(3-Chloro-5-(1H-indol-2-yl)pyridin-4-yl)-2,8-diazaspiro [4.5]decan-1-one (31)

Bromide **11** (173 mg, 502 μmol) and 2-(4,4,5,5-tetramethyl-1,3,2-dioxaborolan-2-yl)-1*H*-indole (134 mg, 551 μmol) were reacted at 120 °C using general synthetic procedure A. The residue was purified by Biotage® FlashMaster Personal$^+$ flash chromatography (DCM ramping to DCM:CH_3OH = 97:3) to give **31** as a beige solid (85 mg, 45%). R_F (DCM:CH_3OH = 94:6) 0.38. m.p. 169–170 °C. ^{1}H NMR (DMSO-d_6) δ 1.26 (app d, 2H, *J* 12.0, CH_2), 1.75 (td, 2H, *J* 12.5 & 3.5, CH_2), 1.83 (t, 2H, *J* 6.5, CH_2), 2.81 (t, 2H, *J* 12.0, CH_2), 3.00–3.20 (m, 4H, 2 × CH_2), 6.54 (s, 1H, indolyl-H), 7.03 (t, 1H, *J* 7.0, indolyl-H), 7.13 (t, 1H, *J* 7.0, indolyl-H), 7.42 (d, 1H, *J* 8.0, indolyl-H), 7.52 (s, 1H, CONH), 7.58 (d, 1H, *J* 8.0, indolyl-H), 8.38 (s, 1H, pyridinyl-H), 8.47 (s, 1H, pyridinyl-H), 11.35 (s, 1H, indolyl-NH). ^{13}C NMR (DMSO-d_6) δ 30.5, 31.8, 37.9, 41.4, 46.6, 102.7, 111.5, 119.5, 120.2, 121.7, 125.4, 127.2, 128.2, 133.4, 136.7, 149.3, 151.0, 152.9, 180.0 (two carbon signals overlapping or obscured). HRMS (ESI+) 381.1483 [M(^{35}Cl)+H]$^+$ & 383.1440 [M(^{37}Cl)+H]$^+$; calcd. for $C_{21}H_{22}ClN_4O^+$ 381.1477 [M(^{35}Cl)+H]$^+$ & 383.1447 [M(^{37}Cl)+H]$^+$. Anal. RP-HPLC Method C: t_R 17.88 min, purity >98%; Method D: t_R 12.72 min, purity >98%.

8-(3-Chloro-5-(1-methyl-1*H*-indol-2-yl)pyridin-4-yl)-2,8-diazaspiro[4.5]decan-1-one (32)

Bromide **11** (173 mg, 502 μmol) and 1-methyl-2-(4,4,5,5-tetramethyl-1,3,2-dioxaborolan-2-yl)-1*H*-indole (194 mg, 754 μmol) were reacted at 140 °C using general synthetic procedure A. The residue was purified by Biotage® FlashMaster Personal$^+$ flash chromatography (DCM ramping to DCM:CH_3OH = 97.5:2.5) to give **32** as a beige solid (25 mg, 13%). R_F (DCM:CH_3OH = 96:4) 0.38. m.p. 129–130 °C. ^{1}H NMR (DMSO-d_6) δ 1.22 (app d, 2H, *J* 12.5, CH_2), 1.65 (t, 2H, *J* 11.5, CH_2), 1.77 (t, 2H, *J* 6.5, CH_2), 2.67 (t, 2H, *J* 12.0, CH_2), 3.06 (t, 2H, *J* 6.5, CH_2), 3.16 (app br s, 2H, CH_2), 3.60 (s, 3H, CH_3), 6.50 (s, 1H, indolyl-H), 7.09 (t, 1H, *J* 7.5, indolyl-H), 7.20 (t, 1H, *J* 7.5, indolyl-H), 7.49 (s, 1H, CONH), 7.50 (d, 1H, *J* 7.5, indolyl-H), 7.59 (d, 1H, *J* 7.5, indolyl-H), 8.25 (s, 1H, pyridinyl-H), 8.53 (s, 1H, pyridinyl-H). ^{13}C NMR (DMSO-d_6) δ 30.7, 30.8, 31.9, 37.8, 41.1, 46.5, 103.2, 110.3, 119.7, 120.3, 121.7, 123.2, 126.4, 127.4, 135.4, 137.3, 150.2, 151.9, 153.8, 179.8 (two carbon signals overlapping or obscured). HRMS (ESI+) 395.1634 [M(^{35}Cl)+H]$^+$ & 397.1611 [M(^{37}Cl)+H]$^+$; calcd. for $C_{22}H_{24}ClN_4O^+$ 395.1633 [M(^{35}Cl)+H]$^+$ & 397.1604 [M(^{37}Cl)+H]$^+$. Anal. RP-HPLC Method C: t_R 19.28 min, purity >95%; Method D: t_R 13.81 min, purity >97%.

8-(3-(1-Benzyl-1*H*-pyrrolo[2,3-*b*]pyridin-3-yl)-5-chloropyridin-4-yl)-2,8-diazaspiro[4.5]decan-1-one (33)

Bromide **11** (173 mg, 502 μmol) and 1-benzyl-3-(4,4,5,5-tetramethyl-1,3,2-dioxaborolan-2-yl)-1*H*-pyrrolo[2,3-*b*]pyridine (190 mg, 568 μmol) were reacted at 120 °C using general synthetic procedure A. The residue was purified by Biotage® FlashMaster Personal$^+$ flash chromatography (DCM ramping to DCM:CH_3OH = 96.5:3.5), and washed with EtOAc (6 mL) to give **33** as a beige solid (120 mg, 51%). R_F (DCM:CH_3OH = 94:6) 0.38. m.p. 252–253 °C. ^{1}H NMR (DMSO-d_6) δ 1.12 (app d, 2H, *J* 12.5, CH_2), 1.53 (t, 2H, *J* 6.5, CH_2), 1.64 (td, 2H, *J* 12.0 & 3.0, CH_2), 2.58 (t, 2H, *J* 12.0, CH_2), 2.98 (app d, 2H, *J* 12.5, CH_2), 3.03 (t, 2H, *J* 6.5, CH_2), 5.56 (s, 2H, phenyl-CH_2), 7.18 (dd, 1H, *J* 7.5 & 4.5, pyrrolopyridinyl-H), 7.22–7.28 (m, 1H, phenyl-H), 7.31–7.33 (m, 4H, 4 × phenyl-H), 7.50 (s, 1H, CONH), 7.72 (s, 1H, pyrrolopyridinyl-H), 7.94 (d, 1H, *J* 7.5, pyrrolopyridinyl-H), 8.29 (s, 1H, pyridinyl-H), 8.35 (d, 1H, *J* 4.0, pyrrolopyridinyl-H), 8.44 (s, 1H, pyridinyl-H). ^{13}C NMR (MSO-d_6) δ 30.2, 31.7, 37.8, 41.3, 46.9, 47.3, 109.3, 116.6, 119.3, 126.1, 127.4, 127.5, 127.6, 128.6, 138.2, 143.4, 147.0, 148.4, 151.3, 153.4, 179.9 (six carbon signals overlapping or obscured). HRMS (ESI+) 472.1896 [M(^{35}Cl)+H]$^+$ & 474.1864 [M(^{37}Cl)+H]$^+$; calcd. for $C_{27}H_{27}ClN_5O^+$ 472.1899 [M(^{35}Cl)+H]$^+$ & 474.1869 [M(^{37}Cl)+H]$^+$. Anal. RP-HPLC Method A: t_R 11.77 min, purity >98%; Method B: t_R 9.22 min, purity >98%.

8-(3-Chloro-5-(1-(phenylsulfonyl)-1*H*-indol-3-yl)pyridin-4-yl)-2,8-diazaspiro[4.5]decan-1-one (34)

Bromide **11** (173 mg, 502 μmol) and 1-(phenylsulfonyl)-3-(4,4,5,5-tetramethyl-1,3,2-dioxaborolan-2-yl)-1*H*-indole (230 mg, 600 μmol) were reacted at 135 °C using general synthetic procedure A. The residue was purified by Biotage® FlashMaster Personal$^+$ flash chromatography (DCM ramping to DCM:CH_3OH = 97.5:2.5) to give **34** as a beige solid (128 mg, 49%). R_F (DCM:CH_3OH = 94:6) 0.46. m.p. 248–249 °C. ^{1}H NMR (DMSO-d_6) δ 0.96 (app d, 2H, *J* 12.5, CH_2), 1.34 (t, 2H, *J* 6.0, CH_2), 1.52 (t, 2H, *J* 10.0, CH_2), 2.33 (t, 2H, *J* 13.0, CH_2), 2.98 (t, 2H, *J* 6.5, CH_2), 3.05 (app d, 2H, *J* 12.5, CH_2), 7.29 (t, 1H, *J* 7.5, indolyl-H), 7.33 (d, 1H, *J* 8.0, indolyl-H), 7.44 (t, 1H, *J* 7.5, indolyl-H), 7.48 (s, 1H, CONH), 7.58 (t, 2H, *J* 7.5, 2 × phenyl-H), 7.69 (t, 1H, *J* 7.5, phenyl-H), 7.96 (s, 1H, indolyl-H), 8.04 (d, 1H, *J* 6.5, indolyl-H), 8.06 (d, 2H, *J* 7.0, 2 × phenyl-H), 8.24 (s, 1H, pyridinyl-H), 8.50 (s, 1H, pyridinyl-H). ^{13}C NMR (DMSO-d_6) δ 30.2, 31.7, 37.7, 41.0, 46.2, 113.6, 120.0, 120.2, 123.5, 124.1, 125.5, 125.6, 126.9, 129.8, 130.8, 134.2, 134.7, 137.0, 149.7, 151.1, 153.5, 179.7 (five carbon signals

overlapping or obscured). HRMS (ESI+) 521.1398 [M(^{35}Cl)+H]$^+$ & 523.1371 [M(^{37}Cl)+H]$^+$; calcd. for $C_{27}H_{26}ClN_4O_3S^+$ 521.1409 [M(^{35}Cl)+H]$^+$ & 523.1379 [M(^{37}Cl)+H]$^+$. Anal. RP-HPLC Method C: t_R 20.26 min, purity >99%; Method D: t_R 15.30 min, purity >98%.

8-(3-Chloro-5-(1*H*-indol-3-yl)pyridin-4-yl)-2,8-diazaspiro [4.5]decan-1-one (35)

Compound **34** (261 mg, 501 μmol) was deprotected using general synthetic procedure C. The residue was purified by Biotage® FlashMaster Personal$^+$ flash chromatography (DCM ramping to DCM:CH_3OH = 95:5) to give **35** as a white solid (152 mg, 80%). R_F (DCM:CH_3OH = 92:8) 0.46. m.p. 245–246 °C. ^{1}H NMR (DMSO-d_6) δ 1.16 (app d, 2H, *J* 12.5, CH_2), 1.55–1.75 (m, 4H, 2 × CH_2), 2.66 (t, 2H, *J* 12.0, CH_2), 2.96–3.12 (m, 4H, 2 × CH_2), 7.05 (t, 1H, *J* 7.5, indolyl-H), 7.16 (t, 1H, *J* 7.5, indolyl-H), 7.41 (d, 1H, *J* 8.5, indolyl-H), 7.43 (s, 1H, indolyl-H or CONH), 7.46 (d, 1H, *J* 8.5, indolyl-H), 7.48 (s, 1H, CONH or indolyl-H), 8.24 (s, 1H, pyridinyl-H), 8.41 (s, 1H, pyridinyl-H), 11.40 (s, 1H, indolyl-NH). ^{13}C NMR (DMSO-d_6) δ 30.3, 31.8, 37.8, 41.4, 46.5, 111.1, 111.9, 118.5, 119.7, 121.7, 125.1, 127.0, 127.1, 127.3, 136.0, 148.1, 151.6, 153.5, 178.0 (two carbon signals overlapping or obscured). HRMS (ESI+) 381.1482 [M(^{35}Cl)+H]$^+$ & 383.1439 [M(^{37}Cl)+H]$^+$; calcd. for $C_{21}H_{22}ClN_4O^+$ 381.1477 [M(^{35}Cl)+H]$^+$ & 383.1447 [M(^{37}Cl)+H]$^+$. Anal. RP-HPLC Method C: t_R 15.16 min, purity >98%; Method D: t_R 10.88 min, purity >98%.

8-(3-Chloro-5-(1-(phenylsulfonyl)-1*H*-pyrrolo[2,3-*b*]pyridin-3-yl)pyridin-4-yl)-2,8-diazaspiro[4.5]decan-1-one (36)

Bromide **11** (173 mg, 502 μmol) and 1-(phenylsulfonyl)-3-(4,4,5,5-tetramethyl-1,3,2-dioxaborolan-2-yl)-1*H*-pyrrolo[2,3-*b*] pyridine (212 mg, 552 μmol) were reacted at 120 °C using general synthetic procedure A. The residue was purified by Biotage® FlashMaster Personal$^+$ flash chromatography (DCM ramping to DCM:CH_3OH = 96.5:3.5), and triturated and washed with EtOAc (10 mL) to give **36** as a white solid (45 mg, 17%). R_F (DCM:CH_3OH = 96:4) 0.31. m.p. 252–253 °C. ^{1}H NMR (DMSO-d_6) δ 1.06 (app d, 2H, *J* 12.5, CH_2), 1.45–1.62 (m, 4H, CH_2), 2.50–2.58 (m, 2H, CH_2), 3.04 (t, 2H, *J* 6.5, CH_2), 3.11 (d, 2H, *J* 12.5, CH_2), 7.33 (dd, 1H, *J* 7.0 & 5.5, pyrrolopyridinyl-H), 7.50 (s, 1H, CONH), 7.61 (t, 2H, *J* 7.5, 2 × phenyl-H), 7.71 (t, 1H, *J* 7.5, phenyl-H), 7.89 (d, 1H, *J* 7.5, pyrrolopyridinyl-H), 8.05 (s, 1H, pyrrolopyridinyl-H), 8.17 (d, 2H, *J* 7.5, 2 × phenyl-H), 8.31 (s, 1H, pyridinyl-H), 8.45 (d, 1H, *J* 4.5, pyrrolopyridinyl-H), 8.50 (s, 1H, pyridinyl-H). ^{13}C NMR (DMSO-d_6) δ 30.5, 31.8, 37.8, 41.0, 46.6, 116.2, 119.9, 122.6, 123.8, 125.4, 127.1, 127.6, 129.3, 129.7, 134.8, 137.4, 145.5, 146.6, 149.9, 151.1, 153.5, 179.8 (four carbon signals overlapping or obscured). HRMS (ESI+) 522.1347 [M(^{35}Cl)+H]$^+$ & 524.1318 [M(^{37}Cl)+H]$^+$; calcd. for $C_{26}H_{25}ClN_5O_3S^+$ 522.1361 [M(^{35}Cl)+H]$^+$ & 524.1332 [M(^{37}Cl)+H]$^+$. Anal. RP-HPLC Method C: t_R 19.28 min, purity >98%; Method D: t_R 13.80 min, purity >98%.

8-(3-Chloro-5-(1*H*-pyrrolo[2,3-*b*]pyridin-3-yl)pyridin-4-yl)-2,8-diazaspiro[4.5]decan-1-one (37)

Compound **36** (157 mg, 301 μmol) was deprotected using general synthetic procedure C. The residue was purified by Biotage® FlashMaster Personal$^+$ flash chromatography (DCM ramping to DCM:CH_3OH = 92:8) to give **37** as a white solid (86 mg, 75%). R_F (DCM:CH_3OH = 9:1) 0.44. m.p. 297–298 °C. ^{1}H NMR (DMSO-d_6) δ 1.16 (app d, 2H, *J* 12.5, CH_2), 1.63 (td, 2H, *J* 12.0 & 2.5, CH_2), 1.67 (t, 2H, *J* 6.5, CH_2), 2.66 (t, 2H, *J* 12.0, CH_2), 3.05 (t, 2H, *J* 6.5, CH_2), 3.05–3.14 (m, 2H, CH_2), 7.11 (dd, 1H, *J* 7.5 & 4.5, pyrrolopyridinyl-H), 7.48 (s, 1H, CONH), 7.57 (s, 1H, pyrrolopyridinyl-H), 7.85 (d, 1H, *J* 8.0, pyrrolopyridinyl-H), 8.24 (s, 1H, pyridinyl-H), 8.28 (d, 1H, *J* 4.5, pyrrolopyridinyl-H), 8.42 (s, 1H, pyridinyl-H), 11.95 (s, 1H, pyrrolopyridinyl-NH). ^{13}C NMR (DMSO-d_6) δ 30.4, 31.8, 37.9, 41.4, 46.6, 110.0, 116.2, 119.4, 125.5, 126.4, 127.1, 127.2, 143.3, 148.4, 148.5, 151.5, 153.5, 180.0 (two carbon signals overlapping or obscured). HRMS (ESI+) 382.1429 [M(^{35}Cl)+H]$^+$ & 384.1403 [M(^{37}Cl)+H]$^+$; calcd. for $C_{20}H_{21}ClN_5O^+$ 382.1429 [M(^{35}Cl)+H]$^+$ & 384.1400 [M(^{37}Cl)+H]$^+$. Anal. RP-HPLC Method C: t_R 15.86 min, purity >98%; Method D: t_R 9.38 min, purity >98%.

8-(3-(Benzofuran-2-yl)-5-chloropyridin-4-yl)-2,8-diazaspiro [4.5]decan-1-one (38)

Bromide **11** (173 mg, 502 μmol) and 2-(benzofuran-2-yl)-4,4,5,5-tetramethyl-1,3,2-dioxaborolane (129 mg, 528 μmol) were reacted at 130 °C using general synthetic procedure A. The residue was purified by Biotage® FlashMaster Personal$^+$ flash chromatography (DCM ramping to DCM:CH_3OH = 97:3) to give **38** as a white solid (65 mg, 34%). R_F (DCM:CH_3OH = 95:5) 0.33. m.p. 177–178 °C. ^{1}H NMR (DMSO-d_6) δ 1.32 (app d, 2H, *J* 12.5, CH_2), 1.79 (td, 2H, *J* 12.5 & 4.0, CH_2), 1.89 (t, 2H, *J* 6.5, CH_2), 2.84 (t, 2H, *J* 11.5, CH_2), 3.06–3.22 (m, 2H, CH_2), 3.13 (t, 2H, *J* 6.5, CH_2), 7.23 (s, 1H, benzofuranyl-H), 7.30 (td, 1H, *J* 7.0 & 0.5, benzofuranyl-H), 7.37 (td, 1H, *J* 7.0 & 1.0, benzofuranyl-H), 7.55 (br s, 1H, CONH), 7.66 (d, 1H, *J* 8.0, benzofuranyl-H), 7.72 (d, 1H, *J* 7.5, benzofuranyl-H), 8.55 (s, 2H, 2 × pyridinyl-H). ^{13}C NMR (DMSO-d_6) δ 30.4, 31.8, 37.9, 41.4, 46.1, 106.0, 111.4, 121.6, 122.9, 123.4, 125.1, 128.1, 128.6, 150.3, 150.8, 151.8, 153.0, 154.6, 180.0 (two carbon signals overlapping or obscured). HRMS (ESI+) 382.1322 [M(^{35}Cl)+H]$^+$ & 384.1297 [M(^{37}Cl)+H]$^+$; calcd. for $C_{21}H_{21}ClN_3O_2^+$ 382.1317 [M(^{35}Cl)+H]$^+$ & 384.1287 [M(^{37}Cl)+H]$^+$. Anal. RP-HPLC Method A: t_R 12.25 min, purity >95%; Method B: t_R 10.34 min, purity >95%.

8-(3-(Benzo[*b*]thiophen-2-yl)-5-chloropyridin-4-yl)-2,8-diazaspiro[4.5]decan-1-one (39)

Bromide **11** (173 mg, 502 μmol) and benzo[*b*]thiophen-2-ylboronic acid (94.0 mg, 528 μmol) were reacted at 130 °C using general synthetic procedure A. The residue was purified by Biotage® FlashMaster Personal$^+$ flash chromatography (DCM ramping to DCM:CH_3OH = 97:3) to give **39** as a white solid (70 mg, 35%). R_F (DCM:CH_3OH = 95:5) 0.33. m.p. 230–232 °C. ^{1}H NMR (DMSO-d_6) δ 1.32 (app d, 2H, *J* 12.5, CH_2), 1.85 (td, 2H, *J* 12.0 & 3.0, CH_2), 1.90 (t, 2H, *J* 7.0, CH_2), 2.98 (t, 2H, *J* 11.0, CH_2), 3.05–3.22 (m, 2H, CH_2), 3.12 (t, 2H, *J* 6.5, CH_2), 7.40 (td, 1H, *J* 7.0 & 1.5, benzothiophenyl-H), 7.43 (td, 1H, *J* 7.0 & 1.5, benzothiophenyl-H), 7.54 (s, 1H, CONH), 7.65 (s, 1H, benzothiophenyl-H), 7.91 (d, 1H, *J* 7.0, benzothiophenyl-H), 8.01 (d, 1H, *J* 7.0, benzothiophenyl-H), 8.51 (s, 1H, pyridinyl-H), 8.53 (s, 1H, pyridinyl-H). ^{13}C NMR (DMSO-d_6) δ 30.4, 31.5, 37.9, 41.3, 46.6, 122.4, 124.0, 124.5, 124.9, 125.0, 127.5, 128.1, 137.8, 139.4, 140.2, 150.0, 150.7, 152.7, 180.1 (two carbon signals overlapping or obscured). HRMS (ESI+) 398.1086 [M(^{35}Cl)+H]$^+$ & 400.1068 [M(^{37}Cl)+H]$^+$; calcd. for $C_{21}H_{21}ClN_3OS^+$ 398.1088 [M(^{35}Cl)+H]$^+$ & 400.1059 [M(^{37}Cl)+H]$^+$. Anal. RP-HPLC Method A: t_R 12.42 min, purity >97%; Method B: t_R 10.56 min, purity >99%.

8-(3-(Benzofuran-3-yl)-5-chloropyridin-4-yl)-2,8-diazaspiro [4.5]decan-1-one (40)

Bromide **11** (173 mg, 502 μmol) and 2-(benzofuran-3-yl)-4,4,5,5-tetramethyl-1,3,2-dioxaborolane (135 mg, 553 μmol) were reacted at 120 °C using general synthetic procedure A. The residue was purified by Biotage® FlashMaster Personal$^+$ flash chromatography (DCM ramping to DCM:CH_3OH = 97.5:2.5), and crystallised with EtOAc/*n*-hexane to give **40** as a beige solid (67 mg, 35%). R_F (DCM:CH_3OH = 94:6) 0.40. m.p. 185–186 °C. ^{1}H NMR (DMSO-d_6) δ 1.18 (app d, 2H, *J* 12.5, CH_2), 1.64 (td, 2H, *J* 12.0 & 2.5, CH_2), 1.67 (t, 2H, *J* 6.5, CH_2), 2.74 (t, 2H, *J* 12.0, CH_2), 3.05 (t, 2H, *J* 6.5, CH_2), 3.16 (d, 2H, *J* 12.5, CH_2), 7.31 (t, 1H, *J* 7.5, benzofuranyl-H), 7.40 (t, 1H, *J* 7.5, benzofuranyl-H), 7.48 (s, 1H, CONH), 7.50 (d, 1H, *J* 8.0, benzofuranyl-H), 7.68 (d, 1H, *J* 8.5, benzofuranyl-H), 8.15 (s, 1H, benzofuranyl-H), 8.27 (s, 1H, pyridinyl-H), 8.50 (s, 1H, pyridinyl-H). ^{13}C NMR (DMSO-d_6) δ 30.4, 31.8, 37.8, 41.3, 46.7, 111.8, 117.4, 120.0, 122.7, 123.5, 125.1, 127.0, 127.7, 144.1, 149.8, 151.1, 153.6, 154.5, 179.9 (two carbon signals overlapping or obscured). HRMS (ESI+) 382.1319 [M(^{35}Cl)+H]$^+$ & 384.1293 [M(^{37}Cl)+H]$^+$; calcd. for $C_{21}H_{21}ClN_3O_2^+$ 382.1317 [M(^{35}Cl)+H]$^+$ & 384.1287 [M(^{37}Cl)+H]$^+$. Anal. RP-HPLC Method C: t_R 19.76 min, purity >99%; Method D: t_R 12.90 min, purity >99%.

8-(3-(Benzo[*b*]thiophen-3-yl)-5-chloropyridin-4-yl)-2,8-diazaspiro[4.5]decan-1-one (41)

Bromide **11** (173 mg, 502 μmol) and benzo[*b*]thiophen-3-ylboronic acid (94.0 mg, 528 μmol) were reacted at 120 °C using general synthetic procedure A. The residue was purified by Biotage® FlashMaster Personal$^+$ flash chromatography (DCM ramping to DCM:CH_3OH = 97:3), and crystallised with DCM/EtOAc to give **41** as a grey solid (110 mg, 55%). R_F (DCM:CH_3OH = 95:5) 0.30. m.p. 156–157 °C. ^{1}H NMR (DMSO-d_6) δ 1.11 (app d, 2H, *J* 13.0, CH_2), 1.50–1.65 (m, 2H, CH_2), 1.58 (t, 2H, *J* 7.0, CH_2), 2.50–2.60 (m, 2H, CH_2), 3.02 (t, 2H, *J* 7.0, CH_2), 3.07 (app d, 2H, *J* 12.5, CH_2), 7.41 (td, 1H, *J* 7.0 & 1.0, benzothiophenyl-H), 7.45 (td, 1H, *J* 7.0 & 1.0, benzothiophenyl-H), 7.47 (s, 1H, CONH), 7.50 (dd, 1H, *J* 7.0 & 1.0, benzothiophenyl-H), 7.79 (s, 1H, benzothiophenyl-H), 8.08 (d, 1H, *J* 7.0, benzothiophenyl-H), 8.22 (s, 1H, pyridinyl-H), 8.53 (s, 1H, pyridinyl-H). ^{13}C NMR (DMSO-d_6) δ 30.3, 31.7, 37.7, 41.2, 46.5, 122.4, 123.2, 124.8, 124.9, 126.6, 126.7, 127.0, 132.3, 138.8, 139.2, 149.6, 150.9, 153.7, 179.7 (two carbon signals overlapping or obscured). HRMS (ESI+) 398.1090 [M(^{35}Cl)+H]$^+$ & 400.1059 [M(^{37}Cl)+H]$^+$; calcd. for $C_{21}H_{21}ClN_3OS^+$ 398.1088 [M(^{35}Cl)+H]$^+$ & 400.1059 [M(^{37}Cl)+H]$^+$. Anal. RP-HPLC Method A: t_R 11.82 min, purity >96%; Method B: t_R 9.39 min, purity >97%.

4.2. Biology

Kinase Assays. A radiometric protein kinase assay—^{33}PanQinase® Activity Assay—was used to measure the residual kinase activity of CDK8/cyclin C. The assay was performed in a 96-well FlashPlate™ from PerkinElmer (Boston, MA, USA) in a reaction volume of 50 μL on a Beckman Coulter/SAGIAN™ Core System. A reaction cocktail was formed by pipetting the following four solutions in an order of [i] 20 μL of assay buffer (standard buffer), [ii] 5 μL of ATP solution (in H_2O), [iii] 5 μL of a test compound (in 10% DMSO) [iv] 10 μL of enzyme (*i.e.*, CDK8), solution & 10 μL of substrate (*i.e.*, RBER-IRStide) solution (premixed). Each well contained 70 mM HEPES-NaOH pH 7.5, 3 mM $MgCl_2$, 3 mM $MnCl_2$, 3 μM sodium orthovanadate, 1.2 mM dithiothreitol (DTT), 50 μg/mL polyethylene glycol (PEG) 20000, 1.0 μM ATP (the concentration corresponded to the apparent K_m (ATP) value of CDK8), [γ-^{33}P]-ATP (4–9 × 10^5 cpm per well), 1 ng/μL CDK8 (ProQinase lot: 004), and 20 ng/μL RBER-IRStide (ProQinase lot: 019 or 023). The reaction cocktails were incubated at 30 °C for 60 min. The reactions were stopped with addition of 50 μL of 2% (v/v) H_3PO_4, and plates aspirated and washed twice with 200 μL of 0.9% (w/v) NaCl. Incorporation of $^{33}P_i$ was determined with a microplate scintillation counter (Microbeta, Wallace). A residual kinase activity (%) at each compound concentration and an IC_{50} value of a test compound were calculated using Quattro Workflow V3.1.1 (Quattro Research GmbH, Münich, Germany; www.quattro-research.com). The fitting model used for the IC_{50} determination was sigmoidal dose-response (variable slope) with the parameters of TOP and BOTTOM fixed at 100% and 0%, respectively. The method of least squares was used for regression analysis. Residual kinase activities (%) of the kinases except CDK8 in the presence of 1 μM **38** or **39** and IC_{50} values of the two compounds against GSK-3α/β and PCK-θ were determined using Eurofins Scientific's KinaseProfiler™ kinase screening and profiling service (key details of the service can be found at https://www.eurofinsdiscoveryservices.com/services/in-vitro-assays/kinases/kinase-profiler/) or by HotSpot™ radioisotope-based kinase assays at Reaction Biology Corporation (the assay protocol is available at https://www.reactionbiology.com/services/target-specific-assays/kinase-assays/kinase-screening). All of the IC_{50} values determined by three contract research organisations were converted to the K_i values using the Cheng-Prusoff equation: $K_i = IC_{50}/(1+([ATP]/K_m(ATP)))$, where [ATP] is the concentration of ATP used for the IC_{50} determination and K_m (ATP) for each kinase is determined experimentally [62].

Cell Culture. All the cell lines were obtained from the cell bank at Drug Discovery and Development, University of South Australia. Each of them was cultured, according to the American Type Culture Collection (ATCC) recommendation, in Roswell Park Memorial Institute (RPMI)-1640, Dulbecco's Modified Eagle's Medium (DMEM), or Minimum Essential Media (MEM), with 10% foetal bovine serum (FBS, Sigma-Aldrich, Castle Hill, NSW, Australia) within a humidified incubator at 37 °C in the presence of 5% CO_2. No mycoplasma contamination [63] was detected in cell culture.

Cell Viability Assays. MTT (Life Technologies, Mulgrave, Vic, Australia) and resazurin (Sigma-Aldrich) assays were performed with adherent (solid tumour) and suspension (leukaemia) cell lines, respectively, as reported previously [41,50]. Compound concentrations required to inhibit 50% of cell growth (GI_{50}) were calculated using nonlinear regression analysis.

Western Blot Analysis. Western blotting was performed as described previously [64]. Primary antibodies included STAT1, STAT1 with phosphorylated Ser727 (p-STAT1^{S727}) and β-actin (Cell Signaling Technology, Danvers, MA, USA). The anti-rabbit immunoglobulin G (IgG) horseradish peroxidase-conjugated antibody (Cell Signaling Technology) was used as a secondary antibody. Enhanced Chemiluminescence reagents (GE Healthcare Life Sciences, Rydalmere, NSW, Australia) were used for western blot detection.

Profiling of *In Vitro* Drug-like Properties. All of the assays were performed with either **38** or **39** at Cyprotex Discovery Ltd. (Macclesfield, UK). Log $D_{7.4}$ was assessed using the shake flask assay with a buffer at pH 7.4, and pKa acquired with a fast UV spectrometric titration. Aqueous solubility was estimated by turbidimetry. Bidirectional permeability was measured using Caco-2 cell line. Inhibition of CYP450 enzymes and the hERG potassium channel was evaluated using human liver microsomes and CHO-hERG cells, respectively. All the experimental details can be found at https://www.cyprotex.com/services.

Determination of *In Vivo* Pharmacokinetic Properties. Healthy male Sprague-Dawley rats (250–350 g) or male adult BALB/c mice (20–25 g) were allocated into IV- and PO-dosing groups; n = 3–4 per group for rats, and n = 10 per group for mice. Rodents were administered an IV injection of **38** or CCT251545 *via* the tail vein (5 mg/kg for rats, and 2 mg/kg for mice for **38** only), or a single oral dose by gavage (20 mg/kg for rats, and 10 mg/kg for mice for **38** only; 2-h prior fasting was fulfilled). IV formulations consisted of **38** or CCT251545 dissolved in a mixture of 0.1 M sodium acetate buffer (pH 4.5):PEG 400:N-methyl-2-pyrrolidone (5:4:1, v/v/v), and oral formulations were comprised of **38** or CCT251545 dispersed in 1% (w/v) CMC aqueous solution. Blood samples were collected from animals by jugular vein cannula (rats) or cheek bleeding and cardiac puncture under anaesthesia (mice) at time zero and at intervals up to 24 h. Collected blood samples were centrifuged at 7000 *g* for 3 min to separate plasma samples which were stored at −20 °C until analysis. Concentrations of **38** or CCT251545 in plasma samples were quantified using a validated LC/MS/MS method with the AB SCIEX TripleTOF 5600 mass spectrometer. Briefly, plasma samples were supplemented with an internal standard (IS) and extracted with ethyl acetate, and organic phases separated and dried in a Genevac HT-4X HCL centrifugal vacuum evaporator (SP Scientific, Ipswich, UK). The residues were reconstituted in acetonitrile/water (50:50), injected into a Shimadzu Nexera HPLC system, and resolved on a Phenomenex Kinetex Phenyl-Hexyl column (2.6 μm, 100 Å, 50 mm × 2.1 mm) at a mobile phase flow rate of 0.6 mL/min. Mobile phase A was 5% methanol and 0.1% FA in water, and mobile phase B (MPB) 95% methanol and 0.1% FA in water. The mobile phase timetable was set as a linear gradient starting from 2% MPB for 0.5 min, followed by ramping to 100% MPB over 2.3 min and maintaining at 100% MPB

for 1.5 min before returning to 2% MPB for 0.5 min in preparation for the next sample. Ratios of signal areas of compound/IS were obtained from known concentrations of calibrators, and were used to construct a calibration curve which was used to determine the plasma concentrations of the unknown samples. The limit of quantification was 5 ng/mL. The intraday and interday variability for each compound was within ±15%. Non-compartmental analyses of plasma concentration versus time were performed using Phoenix WinNonlin (Certara, St. Louis, MO, USA). These experiments were carried out under the approval of the University of South Australia Animal Ethics Committee (Animal Ethics Number: U21-16).

Assessment of *In Vivo* Toxicity. Female BALB/c nude mice were allocated into three treatment groups of two each, and each group was orally administered **38** at 70 mg/kg, CCT251545 at 70 mg/kg, or vehicle (1% CMC aqueous solution) at 10 mL/kg once daily for seven consecutive days, and observed for another seven days. One mouse suffered a major, unrelated welfare issue after the first dose of CCT251545, and therefore was humanely killed. Individual body weights were recorded daily (except day 13). On day 15, mice were anaesthetised by inhalation of isoflurane gas, and killed by cervical dislocation without regaining consciousness. Long bones (left femora), lungs, hearts, livers, kidneys, intestines, uteri, ovaries, and brains were collected and fixed in 10% buffered formalin for histopathological examination, and spleens and bone narrows stored in RPMI-1640 containing 10% FBS for FACS analysis. These experiments were carried out under the approval of the University of South Australia Animal Ethics Committee (Animal Ethics Number: 26/13).

Tissues of long bones (left femora), lungs, hearts, livers, kidneys, intestines, uteri, ovaries, and brains were processed, stained and assessed using a histology service at the Hanson Institute of SA Pathology (http://www.hansoninstitute.sa.gov.au/).

Single-cell suspensions of spleens or bone marrows were prepared by mechanical disruption through a 70 μm cell strainer (BD Falcon) into RPMI-1640. Cells were pelleted by centrifugation at 300*g* for 5 min at 4 °C. Red blood cells were lysed by addition of 1 mL per spleen/bone marrow of ammonium-chloride-potassium lysis buffer for 3 min at room temperature. Cells were washed and re-suspended in flow cytometry staining buffer (FACS buffer) at a final concentration of 2×10^7 cells/mL. Approximately 10^6 cells were stained in 50 μL of FACS buffer containing relevant antibodies (CD3 clone 17A2, CD4 clone RM4-5, CD8 clone 53−6.7, CD19 clone ID3, CD11c clone N418, CD11b clone M1/70, Ly6G clone 1A8, Ly6C clone AL-21) for 30−40 min at 4 °C in the dark. Cells were washed twice with FACS buffer, and samples acquired on a BD FACSAria™ Fusion flow cytometer (Becton Dickinson, San Jose, CA).

Declaration of competing interest

The authors declare that they have no known competing financial interests or personal relationships that could have appeared to influence the work reported in this paper.

Acknowledgements

This work was supported by a grant from Yabao Pharmaceutical Group Co., Ltd., China to S.W..

Appendix A. Supplementary data

Supplementary data to this article can be found online at https://doi.org/10.1016/j.ejmech.2021.113248.

References

[1] M. Malumbres, Cyclin-dependent kinases, Genome Biol. 15 (2014). Article number: 122.
[2] J.P. Tassan, M. Jaquenoud, P. Léopold, S.J. Schultz, E.A. Nigg, Identification of human cyclin-dependent kinase 8, a putative protein kinase partner for cyclin C, Proc. Natl. Acad. Sci. U.S.A. 92 (1995) 8871−8875.
[3] V. Leclerc, J.P. Tassan, P.H. O'Farrell, E.A. Nigg, P. Léopold, Drosophila Cdk8, a kinase partner of cyclin C that interacts with the large subunit of RNA polymerase II, Mol. Biol. Cell 7 (1996) 505−513.
[4] S. Philip, M. Kumarasiri, T. Teo, M. Yu, S. Wang, Cyclin-dependent kinase 8: a new hope in targeted cancer therapy? J. Med. Chem. 61 (2018) 5073−5092.
[5] C.J. Fryer, J.B. White, K.A. Jones, Mastermind recruits CycC:CDK8 to phosphorylate the Notch ICD and coordinate activation with turnover, Mol. Cell. 16 (2004) 509−520.
[6] C. Alarcón, A.-I. Zaromytidou, Q. Xi, S. Gao, J. Yu, S. Fujisawa, A. Barlas, A.N. Miller, K. Manova-Todorova, M.J. Macias, G. Sapkota, D. Pan, J. Massagué, Nuclear CDKs drive Smad transcriptional activation and turnover in BMP and TGF-β pathways, Cell 139 (2009) 757−769.
[7] X. Zhao, D. Feng, Q. Wang, A. Abdulla, X.J. Xie, J. Zhou, Y. Sun, E.S. Yang, L.P. Liu, B. Vaitheesvaran, L. Bridges, I.J. Kurland, R. Strich, J.Q. Ni, C. Wang, J. Ericsson, J.E. Pessin, J.Y. Ji, F. Yang, Regulation of lipogenesis by cyclin-dependent kinase 8-mediated control of SREBP-1, J. Clin. Invest. 122 (2012) 2417−2427.
[8] J. Bancerek, Z.C. Poss, I. Steinparzer, V. Sedlyarov, T. Pfaffenwimmer, I. Mikulic, L. Dölken, B. Strobl, M. Müller, D.J. Taatjes, P. Kovarik, CDK8 kinase phosphorylates transcription factor STAT1 to selectively regulate the interferon response, Immunity 38 (2013) 250−262.
[9] A.D. Clark, M. Oldenbroek, T.G. Boyer, Mediator kinase module and human tumorigenesis, Crit. Rev. Biochem. Mol. Biol. 50 (2015) 393−426.
[10] B.L. Allen, D.J. Taatjes, The Mediator complex: a central integrator of transcription, Nat. Rev. Mol. Cell Biol. 16 (2015) 155−166.
[11] R. Firestein, A.J. Bass, S.Y. Kim, I.F. Dunn, S.J. Silver, I. Guney, E. Freed, A.H. Ligon, N. Vena, S. Ogino, M.G. Chheda, P. Tamayo, S. Finn, Y. Shrestha, J.S. Boehm, S. Jain, E. Bojarski, C. Mermel, J. Barretina, J.A. Chan, J. Baselga, J. Tabernero, D.E. Root, C.S. Fuchs, M. Loda, R.A. Shivdasani, M. Meyerson, W.C. Hahn, CDK8 is a colorectal cancer oncogene that regulates β-catenin activity, Nature 455 (2008) 547−551.
[12] A. Kapoor, M.S. Goldberg, L.K. Cumberland, K. Ratnakumar, M.F. Segura, P.O. Emanuel, S. Menendez, C. Vardabasso, G. Leroy, C.I. Vidal, D. Polsky, I. Osman, B.A. Garcia, E. Hernando, E. Bernstein, The histone variant macroH2A suppresses melanoma progression through regulation of CDK8, Nature 468 (2010) 1105−1109.
[13] D. Xu, C.F. Li, X. Zhang, Z. Gong, C.H. Chan, S.W. Lee, G. Jin, A.H. Rezaeian, F. Han, J. Wang, W.L. Yang, Z.Z. Feng, W. Chen, C.Y. Wu, Y.J. Wang, L.P. Chow, X.F. Zhu, Y.X. Zeng, H.K. Lin, Skp2-macroH2A1-CDK8 axis orchestrates G2/M transition and tumorigenesis, Nat. Commun. 6 (2015). Article number: 6641.
[14] H.E. Pelish, B.B. Liau, I.I. Nitulescu, A. Tangpeerachaikul, Z.C. Poss, D.H. Da Silva, B.T. Caruso, A. Arefolov, O. Fadeyi, A.L. Christie, K. Du, D. Banka, E.V. Schneider, A. Jestel, G. Zou, C. Si, C.C. Ebmeier, R.T. Bronson, A.V. Krivtsov, A.G. Myers, N.E. Kohl, A.L. Kung, S.A. Armstrong, M.E. Lemieux, D.J. Taatjes, M.D. Shair, Mediator kinase inhibition further activates super-enhancer-associated genes in AML, Nature 526 (2015) 273−276.
[15] W. Xu, Z. Wang, W. Zhang, K. Qian, H. Li, D. Kong, Y. Li, Y. Tang, Mutated K-ras activates CDK8 to stimulate the epithelial-to-mesenchymal transition in pancreatic cancer in part via the Wnt/β-catenin signaling pathway, Canc. Lett. 356 (2015) 613−627.
[16] J. Brägelmann, N. Klümper, A. Offermann, A. von Mässenhausen, D. Böhm, M. Deng, A. Queisser, C. Sanders, I. Syring, A.S. Merseburger, W. Vogel, E. Sievers, I. Vlasic, J. Carlsson, O. Andrén, P. Brossart, S. Duensing, M.A. Svensson, Z. Shaikhibrahim, J. Kirfel, S. Perner, Pan-cancer analysis of the Mediator complex transcriptome identifies CDK19 and CDK8 as therapeutic targets in advanced prostate cancer, Clin. Canc. Res. 23 (2017) 1829−1840.
[17] I.B. Roninson, B. Győrffy, Z.T. Mack, A.A. Shtil, M.S. Shtutman, M. Chen, E.V. Broude, Identifying cancers impacted by CDK8/19, Cells 8 (2019) 821−836.
[18] E.M. Putz, D. Gotthardt, G. Hoermann, A. Csiszar, S. Wirth, A. Berger, E. Straka, D. Rigler, B. Wallner, A.M. Jamieson, W.F. Pickl, E.M. Zebedin-Brandl, M. Muller, T. Decker, V. Sexl, CDK8-mediated STAT1-S727 phosphorylation restrains NK cell cytotoxicity and tumor surveillance, Cell Rep. 4 (2013) 437−444.
[19] A. Witalisz-Siepracka, D. Gotthardt, M. Prchal-Murphy, Z. Didara, I. Menzl, D. Prinz, L. Edlinger, E.M. Putz, V. Sexl, NK cell-specific CDK8 deletion enhances antitumor responses, Canc. Immunol. Res. 6 (2018) 458−466.
[20] M.H. Hofmann, R. Mani, H. Engelhardt, M.A. Impagnatiello, S. Carotta, M. Kerenyi, S. Lorenzo-Herrero, J. Böttcher, D. Scharn, H. Arnhof, A. Zoephel, R. Schnitzer, T. Gerstberger, M.P. Sanderson, G. Rajgolikar, S. Goswami, S. Vasu, P. Ettmayer, S. Gonzalez, M. Pearson, D.B. McConnell, N. Kraut, N. Muthusamy, J. Moll, Selective and potent CDK8/19 inhibitors enhance NK-cell activity and promote tumor surveillance, Mol. Canc. Therapeut. 19 (2020) 1018−1030.
[21] V.J. Cee, D.Y. Chen, M.R. Lee, K.C. Nicolaou, Cortistatin A is a high-affinity ligand of protein kinases ROCK, CDK8, and CDK11, Angew. Chem. 48 (2009) 8952−8957.
[22] I.B. Ronnison, D.C. Porter, M.P. Wentland, CDK8-CDK19 Selective Inhibitors and Their Use in Anti-metastatic and Chemopreventative Methods for Cancer, 2014, US20140038958A1.

[23] A. Mallinger, S. Crumpler, M. Pichowicz, D. Waalboer, M. Stubbs, O. Adeniji-Popoola, B. Wood, E. Smith, C. Thai, A.T. Henley, K. Georgi, W. Court, S. Hobbs, G. Box, M.-J. Ortiz-Ruiz, M. Valenti, A. De Haven Brandon, R. TePoele, B. Leuthner, P. Workman, W. Aherne, O. Poeschke, T. Dale, D. Wienke, C. Esdar, F. Rohdich, F. Raynaud, P.A. Clarke, S.A. Eccles, F. Stieber, K. Schiemann, J. Blagg, Discovery of potent, orally bioavailable, small-molecule inhibitors of WNT signaling from a Cell-based pathway screen, J. Med. Chem. 58 (2015) 1717–1735.
[24] T. Dale, P.A. Clarke, C. Esdar, D. Waalboer, O. Adeniji-Popoola, M.-J. Ortiz-Ruiz, A. Mallinger, R.S. Samant, P. Czodrowski, D. Musil, D. Schwarz, K. Schneider, M. Stubbs, K. Ewan, E. Fraser, R. TePoele, W. Court, G. Box, M. Valenti, A. de Haven Brandon, S. Gowan, F. Rohdich, F. Raynaud, R. Schneider, O. Poeschke, A. Blaukat, P. Workman, K. Schiemann, S.A. Eccles, D. Wienke, J. Blagg, A selective chemical probe for exploring the role of CDK8 and CDK19 in human disease, Nat. Chem. Biol. 11 (2015) 973–980.
[25] P. Czodrowski, A. Mallinger, D. Wienke, C. Esdar, O. Poschke, M. Busch, F. Rohdich, S.A. Eccles, M.J. Ortiz-Ruiz, R. Schneider, F.I. Raynaud, P.A. Clarke, D. Musil, D. Schwarz, T. Dale, K. Urbahns, J. Blagg, K. Schiemann, Structure-based optimization of potent, selective, and orally bioavailable CDK8 Inhibitors discovered by high-throughput screening, J. Med. Chem. 59 (2016) 9337–9349.
[26] T. Rzymski, M. Mikula, E. Zylkiewicz, A. Dreas, K. Wiklik, A. Golas, K. Wojcik, M. Masiejczyk, A. Wrobel, I. Dolata, A. Kitlinska, M. Statkiewicz, U. Kuklinska, K. Goryca, L. Sapala, A. Grochowska, A. Cabaj, M. Szajewska-Skuta, E. Gabor-Worwa, K. Kucwaj, A. Bialas, A. Radzimierski, M. Combik, J. Woyciechowski, M. Mikulski, R. Windak, J. Ostrowski, K. Brzozka, SEL120-34A is a novel CDK8 inhibitor active in AML cells with high levels of serine phosphorylation of STAT1 and STAT5 transactivation domains, Oncotarget 8 (2017) 33779–33795.
[27] T. Wang, Z. Yang, Y. Zhang, W. Yan, F. Wang, L. He, Y. Zhou, L. Chen, Discovery of novel CDK8 inhibitors using multiple crystal structures in docking-based virtual screening, Eur. J. Med. Chem. 129 (2017) 275–286.
[28] A. Nakamura, D. Nakata, Y. Kakoi, M. Kunitomo, S. Murai, S. Ebara, A. Hata, T. Hara, CDK8/19 inhibition induces premature G1/S transition and ATR-dependent cell death in prostate cancer cells, Oncotarget 9 (2018) 13474–13487.
[29] J.M. Hatcher, E.S. Wang, L. Johannessen, N. Kwiatkowski, T. Sim, N.S. Gray, Development of highly potent and selective steroidal inhibitors and degraders of CDK8, ACS Med. Chem. Lett. 9 (2018) 540–545.
[30] E. Solum, T.V. Hansen, R. Aesoy, L. Herfindal, New CDK8 inhibitors as potential anti-leukemic agents - design, synthesis and biological evaluation, Bioorg. Med. Chem. 28 (2020) 115461–115468.
[31] A. Mallinger, K. Schiemann, C. Rink, J. Sejberg, M.A. Honey, P. Czodrowski, M. Stubbs, O. Poeschke, M. Busch, R. Schneider, D. Schwarz, D. Musil, R. Burke, K. Urbahns, P. Workman, D. Wienke, P.A. Clarke, F.I. Raynaud, S.A. Eccles, C. Esdar, F. Rohdich, J. Blagg, 2,8-Disubstituted-1,6-naphthyridines and 4,6-disubstituted-isoquinolines with potent, selective affinity for CDK8/19, ACS Med. Chem. Lett. 7 (2016) 573–578.
[32] M.F.T. Koehler, P. Bergeron, E.M. Blackwood, K. Bowman, K.R. Clark, R. Firestein, J.R. Kiefer, K. Maskos, M.L. McCleland, L. Orren, L. Salphati, S. Schmidt, E.V. Schneider, J. Wu, M.H. Beresini, Development of a potent, specific CDK8 kinase inhibitor which phenocopies CDK8/19 knockout cells, ACS Med. Chem. Lett. 7 (2016) 223–228.
[33] X. Han, M. Jiang, C. Zhou, Z. Zhou, Z. Xu, L. Wang, A.V. Mayweg, R. Niu, T.G. Jin, S. Yang, Discovery of potent and selective CDK8 inhibitors through FBDD approach, Bioorg. Med. Chem. Lett 27 (2017) 4488–4492.
[34] S. Martínez-González, A.B. García, M.I. Albarrán, A. Cebriá, A. Amezquita-Alves, F.J. García-Campos, J. Martínez-Gago, J. Martínez-Torrecuadrada, I. Muñoz, C. Blanco-Aparicio, J. Pastor, Pyrido[2,3-b][1,5]benzoxazepin-5(6H)-one derivatives as CDK8 inhibitors, Eur. J. Med. Chem. 201 (2020) 112443–112453.
[35] M. Kumarasiri, T. Teo, M. Yu, S. Philip, S.K. Basnet, H. Albrecht, M.J. Sykes, P. Wang, S. Wang, In search of novel CDK8 inhibitors by virtual screening, J. Chem. Inf. Model. 57 (2017) 413–416.
[36] E.V. Schneider, J. Bottcher, R. Huber, K. Maskos, L. Neumann, Structure-kinetic relationship study of CDK8/CycC specific compounds, Proc. Natl. Acad. Sci. U.S.A. 110 (2013) 8081–8086.
[37] Y.N. Imai, Y. Inoue, I. Nakanishi, K. Kitaura, Cl-π interactions in protein-ligand complexes, Protein Sci. 17 (2008) 1129–1137.
[38] X. Jiang, J. Yu, Z. Zhou, J. Kongsted, Y. Song, C. Pannecouque, E. De Clercq, D. Kang, V. Poongavanam, X. Liu, P. Zhan, Molecular design opportunities presented by solvent-exposed regions of target proteins, Med. Res. Rev. 39 (2019) 2194–2238.
[39] S. Lim, P. Kaldis, Cdks, cyclins and CKIs: roles beyond cell cycle regulation, Development 140 (2013) 3079–3093.
[40] C. McInnes, S. Wang, S. Anderson, J. O'Boyle, W. Jackson, G. Kontopidis, C. Meades, M. Mezna, M. Thomas, G. Wood, D.P. Lane, P.M. Fischer, Structural determinants of CDK4 inhibition and design of selective ATP competitive inhibitors, Chem. Biol. 11 (2004) 525–534.
[41] S. Wang, C. Meades, G. Wood, A. Osnowski, S. Anderson, R. Yuill, M. Thomas, M. Mezna, W. Jackson, C. Midgley, G. Griffiths, I. Fleming, S. Green, I. McNae, S.Y. Wu, C. McInnes, D. Zheleva, M.D. Walkinshaw, P.M. Fischer, 2-Anilino-4-(thiazol-5-yl)pyrimidine CDK inhibitors: synthesis, SAR analysis, X-ray crystallography, and biological activity, J. Med. Chem. 47 (2004) 1662–1675.
[42] S. Wang, G. Wood, C. Meades, G. Griffiths, C. Midgley, I. McNae, C. McInnes, S. Anderson, W. Jackson, M. Mezna, R. Yuill, M. Walkinshaw, P.M. Fischer, Synthesis and biological activity of 2-anilino-4-(1H-pyrrol-3-yl) pyrimidine CDK inhibitors, Bioorg. Med. Chem. Lett 14 (2004) 4237–4240.
[43] S. Wang, G. Griffiths, C.A. Midgley, A.L. Barnett, M. Cooper, J. Grabarek, L. Ingram, W. Jackson, G. Kontopidis, S.J. McClue, C. McInnes, J. McLachlan, C. Meades, M. Mezna, I. Stuart, M.P. Thomas, D.I. Zheleva, D.P. Lane, R.C. Jackson, D.M. Glover, D.G. Blake, P.M. Fischer, Discovery and characterization of 2-anilino-4-(thiazol-5-yl)pyrimidine transcriptional CDK inhibitors as anticancer agents, Chem. Biol. 17 (2010) 1111–1121.
[44] H. Shao, S. Shi, D.W. Foley, F. Lam, A.Y. Abbas, X. Liu, S. Huang, X. Jiang, N. Baharin, P.M. Fischer, S. Wang, Synthesis, structure-activity relationship and biological evaluation of 2,4,5-trisubstituted pyrimidine CDK inhibitors as potential anti-tumour agents, Eur. J. Med. Chem. 70 (2013) 447–455.
[45] H. Shao, S. Shi, S. Huang, A.J. Hole, A.Y. Abbas, S. Baumli, X. Liu, F. Lam, D.W. Foley, P.M. Fischer, M. Noble, J.A. Endicott, C. Pepper, S. Wang, Substituted 4-(thiazol-5-yl)-2-(phenylamino)pyrimidines are highly active CDK9 inhibitors: synthesis, X-ray crystal structures, structure-activity relationship, and anticancer activities, J. Med. Chem. 56 (2013) 640–659.
[46] S. Tadesse, M. Yu, L.B. Mekonnen, F. Lam, S. Islam, K. Tomusange, M.H. Rahaman, B. Noll, S.K. Basnet, T. Teo, H. Albrecht, R. Milne, S. Wang, Highly potent, selective, and orally bioavailable 4-thiazol-N-(pyridin-2-yl)pyrimidin-2-amine cyclin-dependent kinases 4 and 6 inhibitors as anticancer drug candidates: design, synthesis, and evaluation, J. Med. Chem. 60 (2017) 1892–1915.
[47] S. Tadesse, G. Zhu, L.B. Mekonnen, J.L. Lenjisa, M. Yu, M.P. Brown, S. Wang, A novel series of N-(pyridin-2-yl)-4-(thiazol-5-yl)pyrimidin-2-amines as highly potent CDK4/6 inhibitors, Future Med. Chem. 9 (2017) 1495–1506.
[48] S. Tadesse, L. Bantie, K. Tomusange, M. Yu, S. Islam, N. Bykovska, B. Noll, G. Zhu, P. Li, F. Lam, M. Kumarasiri, R. Milne, S. Wang, Discovery and pharmacological characterization of a novel series of highly selective inhibitors of cyclin-dependent kinases 4 and 6 as anticancer agents, Br. J. Pharmacol. 175 (2018) 2399–2413.
[49] X. Han, M. Jiang, A.V. Mayweg, L. Wang, S. Yang, Novel Pyrrole Derivatives for the Treatment of Cancer, 2014, WO2014154723A1.
[50] M. Yu, P. Li, S.K. Basnet, M. Kumarasiri, S. Diab, T. Teo, H. Albrecht, S. Wang, Discovery of 4-(dihydropyridinon-3-yl)amino-5-methylthieno[2,3-d]pyrimidine derivatives as potent Mnk inhibitors: synthesis, structure-activity relationship analysis and biological evaluation, Eur. J. Med. Chem. 95 (2015) 116–126.
[51] A. Mallinger, K. Schiemann, C. Rink, F. Stieber, M. Calderini, S. Crumpler, M. Stubbs, O. Adeniji-Popoola, O. Poeschke, M. Busch, P. Czodrowski, D. Musil, D. Schwarz, M.-J. Ortiz-Ruiz, R. Schneider, C. Thai, M. Valenti, A. de Haven Brandon, R. Burke, P. Workman, T. Dale, D. Wienke, P.A. Clarke, C. Esdar, F.I. Raynaud, S.A. Eccles, F. Rohdich, J. Blagg, Discovery of potent, selective, and orally bioavailable small-molecule modulators of the Mediator complex-associated kinases CDK8 and CDK19, J. Med. Chem. 59 (2016) 1078–1101.
[52] P.A. Clarke, M.J. Ortiz-Ruiz, R. TePoele, O. Adeniji-Popoola, G. Box, W. Court, S. Czasch, S. El Bawab, C. Esdar, K. Ewan, S. Gowan, A. De Haven Brandon, P. Hewitt, S.M. Hobbs, W. Kaufmann, A. Mallinger, F. Raynaud, T. Roe, F. Rohdich, K. Schiemann, S. Simon, R. Schneider, M. Valenti, S. Weigt, J. Blagg, A. Blaukat, T.C. Dale, S.A. Eccles, S. Hecht, K. Urbahns, P. Workman, D. Wienke, Assessing the mechanism and therapeutic potential of modulators of the human Mediator complex-associated protein kinases, eLife 5 (2016), e20722.
[53] J. Bancerek, Z.C. Poss, I. Steinparzer, V. Sedlyarov, T. Pfaffenwimmer, I. Mikulic, L. Dolken, B. Strobl, M. Muller, D.J. Taatjes, P. Kovarik, CDK8 kinase phosphorylates transcription factor STAT1 to selectively regulate the interferon response, Immunity 38 (2013) 250–262.
[54] L. Di, E.H. Kerns, Profiling drug-like properties in discovery research, Curr. Opin. Chem. Biol. 7 (2003) 402–408.
[55] E.H. Kerns, L. Di, Automation in pharmaceutical profiling, J. Assoc. Lab. Autom. 10 (2005) 114–123.
[56] M. Yu, S. Tadesse, S. Wang, USFDA-approved small-molecule kinase inhibitors for cancer therapy, in: D.J. Abraham (Ed.) Burger's Medicinal Chemistry, Drug Discovery and Development (eighth ed.), John Wiley and Sons Ltd., Hoboken, in press.
[57] R.S. Obach, R.L. Walsky, K. Venkatakrishnan, E.A. Gaman, J.B. Houston, L.M. Tremaine, The utility of in vitro cytochrome P450 inhibition data in the prediction of drug-drug interactions, J. Pharmacol. Exp. Therapeut. 316 (2006) 336–348.
[58] N. Ferri, P. Siegl, A. Corsini, J. Herrmann, A. Lerman, R. Benghozi, Drug attrition during pre-clinical and clinical development: understanding and managing drug-induced cardiotoxicity, Pharmacol. Ther. 138 (2013) 470–484.
[59] P.J. Webborn, The role of pharmacokinetic studies in drug discovery: where are we now, how did we get here and where are we going? Future Med. Chem. 6 (2014) 1233–1235.
[60] C. Hall, E. Lueshen, A. Mošat, A.A. Linninger, Interspecies scaling in pharmacokinetics: a novel whole-body physiologically based modeling framework to discover drug biodistribution mechanisms in vivo, J. Pharm. Sci. 101 (2012) 1221–1241.
[61] M. Chen, J. Li, J. Liang, Z.S. Thompson, K. Kathrein, E.V. Broude, I.B. Roninson, Systemic toxicity reported for CDK8/19 inhibitors CCT251921 and MSC2530818 is not due to target inhibition, Cells 8 (2019) 1413–1429.
[62] Y. Cheng, W.H. Prusoff, Relationship between the inhibition constant (KI) and the concentration of inhibitor which causes 50 per cent inhibition (I50) of an enzymatic reaction, Biochem. Pharmacol. 22 (1973) 3099–3108.
[63] L. Nikfarjam, P. Farzaneh, Prevention and detection of Mycoplasma contamination in cell culture, Cell J 13 (2012) 203–212.
[64] T. Teo, M. Yu, Y. Yang, T. Gillam, F. Lam, M.J. Sykes, S. Wang, Pharmacologic co-inhibition of Mnks and mTORC1 synergistically suppresses proliferation and perturbs cell cycle progression in blast crisis-chronic myeloid leukemia cells, Canc. Lett. 357 (2015) 612–623.